POLITECHNIKA WARSZAWSKA

Application of Image Processing in Flow Visualization of Vortex Flow Meter

Author: Javier Gogorcena

Advisor: dr inż. Zbigniew M. Wawrzyniak,PhD

Warsaw University of Technology

September 2009 – February 2010

TABLE OF CONTENTS

1. ABSTRACT

This project presents a method for obtaining qualitative and quantitative results using flow visualization as a way of analyzing the Kármán vortex street phenomena. In the specific case of this investigation, two different fluid flows were analyzed where trajectory and convection velocity of flow vortices could be calculated. As the method of visualization was used, 8 pictures of each of the two flows were taken in order to post-process them using CAD tools. Red and blue markers were injected to the fluid to make the image processing easier. The computer processing allowed the investigator to improve the quality of the pictures and find the center of gravity of each of the whirls. The trajectory of the whirls was analyzed and it was concluded that the movement of the whirls was not in a straight line. The whirls were moving with the fluid current but with some angle from the flow original direction. The convection velocity was also analyzed and it was concluded that in the close neighborhood of the bluff body the vortices were moving slower than at a greater distance. This result confirms the results obtained by simulation and by other investigations.

Este proyecto presenta un método para obtener información cualitativa y cuantitativa usando el método de visualización de flujo para analizar el fenómeno de Kárman vortex street. En el caso específico de esta investigación, dos flujos de un fluido fueron analizados donde la trayectoria y la velocidad de los vórtices pudieron ser calculadas. Como se utilizó el método de visualización, 8 fotografías de cada uno de los flujos fueron tomadas para poder ser post-procesadas utilizando herramientas CAD. Unos marcadores rojos y azules fueron inyectados en el fluido para facilitar el procesado de imagen. El procesado por ordenador permitió al investigador mejorar la calidad de las imágenes y encontrar el centro de gravedad de los vórtices. La trayectoria de los vórtices fue analizada y se concluyó que su movimiento no era en línea recta. Los remolinos se movían con la corriente del fluido pero con un cierto ángulo con respecto a la dirección original del flujo. La velocidad fue también analizada y se concluyó que en las cercanías del origen los vórtices se movían más despacio que a una distancia más lejana. Este resultado confirma los resultados anteriormente obtenidos por simulación y por otras investigaciones.

2. INTRODUCTION

The vortex flow meter is based on the well-known von Karman vortex street phenomenon. This phenomenon consists on a double row of line vortices in a fluid. Under certain conditions a Kármán vortex street is shed in the wake of bluff cylindrical bodies when the relative fluid velocity is perpendicular to the generators of the cylinder (Figure 2.1). This periodic shedding of eddies occurs first from one side of the body and then from the other, an unusual phenomenon because the oncoming flow may be perfectly steady. Vortex streets can often be seen, for example, in rivers downstream of the columns supporting a bridge. They can be created by steady winds blowing past smokestacks, transmission lines, bridges, missiles about to be launched vertically, and pipelines aboveground in the desert.

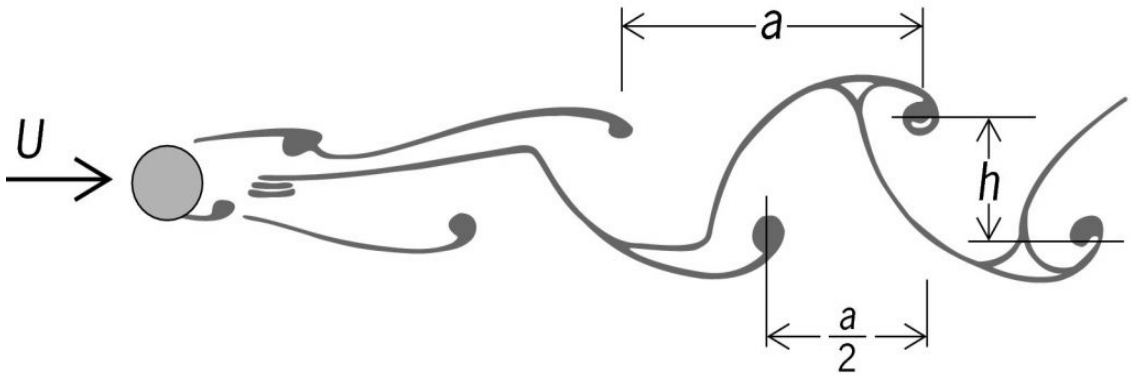

Figure 2.1 – Kármán Vortex street phenomenon

It is obvious, that each successful meter design is determined by comprehensive understanding of applied physical phenomena. Von Karman vortex street phenomenon is very complex and sensitive on numerous physical factors. Hence, the necessity of investigations with application of miscellaneous methods. Determination of the vortex convection is aimed at the deeper understanding of the phenomena.

The vortex method has been widely used and it is still promising for making flow measurements. The vortex flow meter remains very attractive for industrial applications due to its high accuracy, insensitivity to the physical properties of the medium and linear dependence on frequency versus flow rate. The frequency of generated vortices is linear as the function of flow velocity:

$$f = S_T \frac{v}{d}$$

where S_T is the Strouhal number, v the fluid velocity and d is the bluff body diameter.The Strouhal number S_T is constant over a very wide range of flow velocities. In spite of the very simple equation, which describes the behavior of the vortex flowmeter, the phenomena appearing in the meter are very complicated, and many unidentified factors may influence the vortex shedding. Hence, a complete description of these phenomena is not feasible, necessitating further research. Various research methods must be applied to obtain a more complete understanding of the phenomena, with each method elucidating partial information.

3. PROBLEM DESCRIPTION

The problem of the convection velocity of vortices is very interesting, although almost never was present in the papers and articles related to the vortex meter. The first approach to von Karman vortex street description – known from the literature – is based on supposition, that vortices are transported by the flowing fluid and their velocity is equal to the fluid velocity. Only results of simulation of the analytical model [2,3] performed by Pankanin et al. show, that the velocity is not stable, but – on the contrary – its considerable changes in the closest neighborhood of the bluff body are observed. The model concerns the vortex development vs. distance from its origin. The idea of the model is shown in Figure 2.2

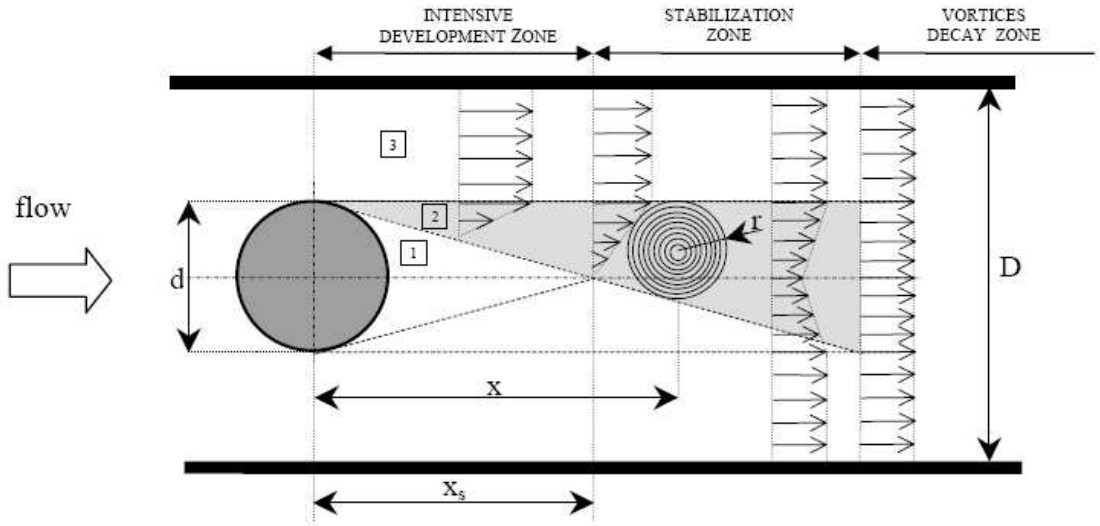

Figure 3.1 – Development of vortex as its distance from the origin grows

The concept of the model is based on the existence of the "low motion" area in the close neighborhood downstream the bluff body. This area called later the "stagnation region" has been suggested by Birkhoff [4-6] as a factor being conducive to vortex generation. It is worth to mention, that the existence of the stagnation region has been confirmed by the laboratory investigations [7]. In the model, eddies arise on the bluff body surface in the area of boundary layer separation. Then they grow-up rolling downstream on the surface of the stagnation region. Succeeding layers are added to the vortex, hence its diameter and energy increase.

3.1 SIMULATION

The first important results regarding the calculation of the convection velocity of the vortices are the results obtained by simulation. Due to simulation of the phenomenon using the model, the changeability of the vortex convection velocity was discovered (Figure 2.3).

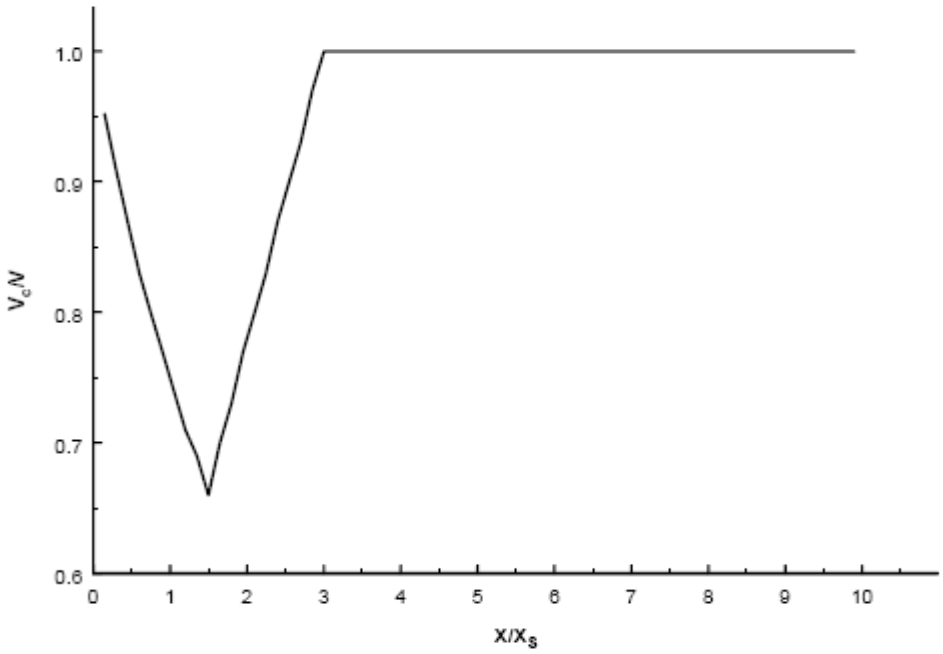

Figure 3.2 – Simulation normalized results of convection velocity vs distance from the bluff body

As it is seen, the convection velocity of the vortices decreases at the beginning and then increases to the stable value equal to the axial velocity of the flowing fluid. It should be mentioned here, that this model has been performed for circular cylinder as the bluff body.

In the assumed model (Figure 3.1) – described in detail in [2] – the convection velocity decrease results from the stagnation region appearance just downstream the bluff body.

3.2 PREVIOUS INVESTIGATIONS

Two previous investigations were presented to the author of this project before starting it. The first one was intended to be a reference so similar results could be obtained, and it was presented in [1]. In this mentioned investigation, flow visualization tests were carried out for circular cylinder bluff bodies (10 mm and 12 mm diameter) with slits. Convection velocity values were calculated and the results can be observed on Figure 3.3. The results found on these observations were very close to the ones expected from simulation so it could be

concluded that in the close neighborhood of the bluff body the vortices move slower than at a greater distance from their origin.

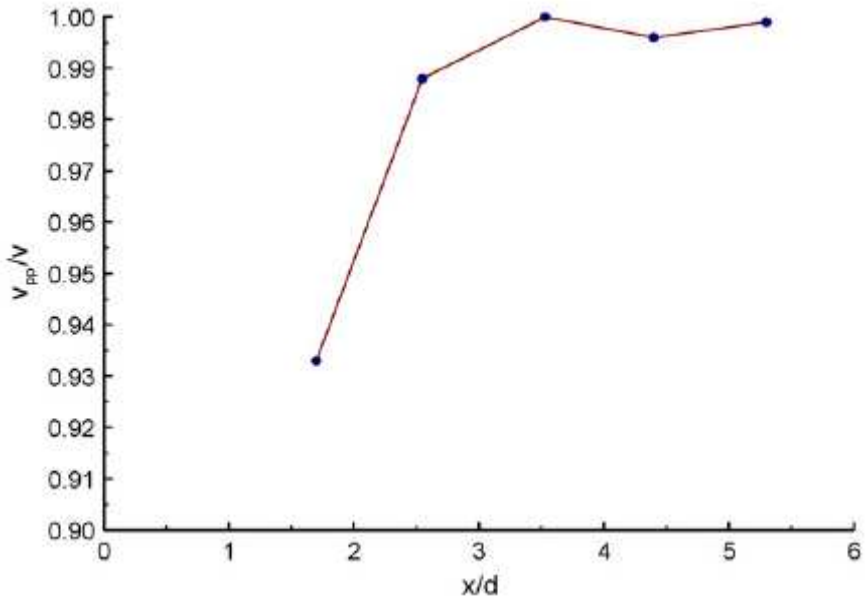

Figure 3.3 – Convection velocity vs distance from the bluff body obtained by experimentation

The second investigation presented to the author of this work was an algorithm designed for analyzing set of pictures similar to the ones explained and processed in subsequent sections of this report. The main objective of this project was to improve and fix this algorithm so more reliable and clear results can be obtained.

4. PROCESS OF VISUALIZATION

The results of this project were obtained after an investigation that needed several steps. As it has been mentioned before in this report, the procedure consisted on flow visualization and image processing. Visualization has been widely used throughout history by many investigators to obtain results that most of the times were as accurate as the ones obtained from computer simulations or experimental procedures.

4.1 FLOW VISUALIZATION

4.1.1 DEFINITION AND HISTORY

Nakayama [8] defines visualization as "an interdisciplinary imaging technique devoted to make the invisible visible by the techniques of experimental and computer-aided simulations". Visualization has been one of the most used techniques to analyze different phenomena that were not possible to be processed by other ways. A special example of this is the flow visualization. It is believed that the man that took the first scientific approach was Leonardo da Vinci, who sat by the river side and observed the vortices shedding on the sharp edges turning up the river. Sketches and notes were found (Figure 4.1) that showed how Da Vinci investigated many kinds of flows by visualization, including flows around obstacles or vortices of divergent flow.

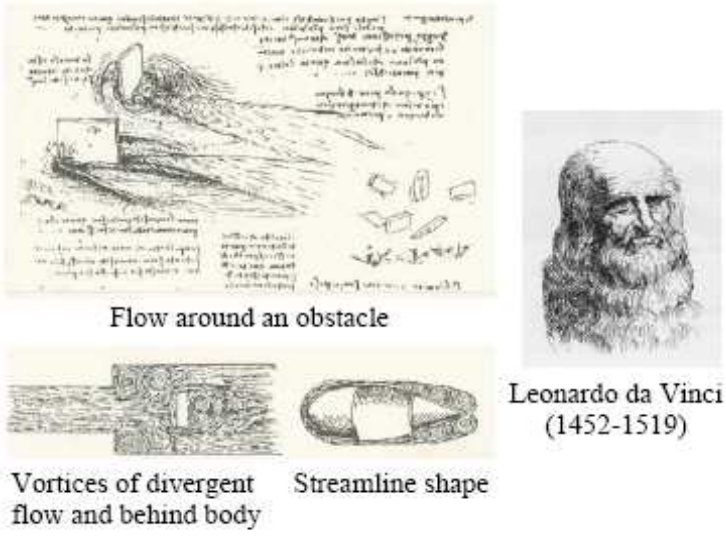

Figure 4.1 – Flow investigations by Leonardo Da Vinci

Osborne Reynolds, and English scientist and engineer, made a great discovery by clarifying the transition phenomena from laminar to turbulent flow. Subsequently, most of the principal discoveries on fluid phenomena were made through visualization, such as the study of high-velocity air flow by Ernst Mach, an Austrian physicist and philosopher, the advocacy of boundary layer by Ludwig Prandtl, a German physicist, the discovery of bursting phenomena in the generating mechanism of turbulence by Stephen Kline, an American engineer, and of course the well known elucidation of Kármán vortex by Theodor von Kármán.

4.1.2 APPLICATIONS

Visualization is used in many fields of the present world. Although there are an unlimited amount of applications, three simple examples are presented:

- Air flow analysis on wind tunnels by visualization to help design vehicles
- Smoke from volcanoes or wind around buildings visualization to help improve our living environment
- Blood flow observation in order to improve medicine efficiency

4.1.3 EXPANSION

A little diagram (Figure 4.2) is presented below in order to summarize the future view of visualization in the twenty-first century society.

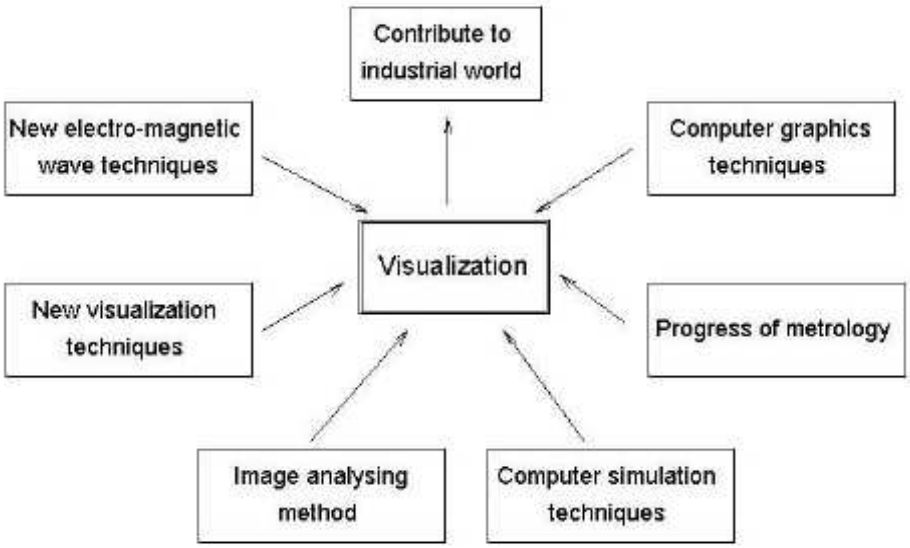

Figure 4.2 – Future view of visualization

4.1.4 APPLICATION TO KARMAN VORTEX STREET FLOW

Visualization has probably been the most important tool in order to analyze vortex street. In fact, von Karman flow visualization experiments led him to the theoretical description of the vortex street. In subsequent decades, researchers of the now known as Karman vortex street, continued using flow visualization in their work. Flow visualization carries many advantages with it, as it enables the whole flow area to be observed. In consequence, various hypotheses were confirmed and numerous accompanying effects were observed.

4.1.5 APPLICATION TO THIS RESEARCH

Very specific equipment was necessary in order to succeed in the process of visualization in this research. Flow visualization investigations have been carried out on a specialized module represented on Figure 4.3. The specially designed chamber is the main part of the module and the chamber construction ensures an even flow velocity profile in the measuring section. The section is made of 40mm transparent tubing, and it allows for the placement of bluff bodies of various shapes and dimensions. Two various tracers (red and blue) were injected into the flowing fluid through small holes drilled in the bluff body. The outlets of these holes are located near the vortices origin on both sides of the body so the vortices generated on the upper edge of the bluff body are red colored, but the vortices originated on the bottom are blue colored. Due to application of two colors, the further image processing of the pictures is easier and enables obtaining more reliable results.

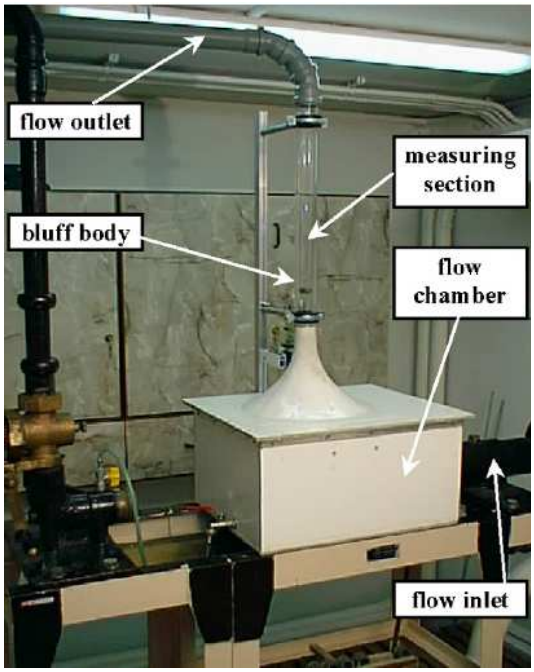

Figure 4.3 – Visualization module for this experiment

Because of the relatively high frequency (for human eyes) of the investigated phenomenon, direct observation is not possible. Only photographs or films enable image analysis. In these investigations, the visualized phenomenon was recorded by a Sony camcorder. Applied fast camera ensures making of series of 8 pictures with chosen intervals.

5. IMAGE PROCESSING

A natural continuation of the process of visualization explained before seems to be the image processing. Very interesting qualitative information might be obtained by direct visualization of the pictures. However, only digital image processing allows extracting quantitative information. The main goal of this post-processing method is to isolate particular vortices as separate objects, and calculate their centers of gravity. Once this is made, calculations such as the whirls' convection velocity, the distance between them or their trajectory through time can be made.

5.1 DIFFERENT METHODS

There are several digital image processing methods that can be used in order to achieve the goals pursued by this investigation. As it was explained before, this goal is no other than isolate the vortices as separate objects to be analyzed later. Therefore, the first thing that should be done is an improvement of the picture quality. Different needs might be found depending on the features of each specific picture (or set of pictures). In particular, the following five improvements are more likely to be needed:

- Contrast increase
- Sharpening of contours
- Elimination of fine random noise
- Smoothing of forms
- Compensation of the influence of particular types of noise

In order to achieve these improvements, some operations are required. It is possible to divide these operations in four groups

5.1.1 Histogram modification

The histogram of a digital image is a table or graph showing the percentage of pixels having certain grey levels. As such, it can be regarded as an estimate of the probabilities of these grey levels. The histogram gives a quick impression of the occupation of these mentioned grey levels. For instance, the histogram of an acquired image shows us whether the adjustments of the camera (e.g. gain, offset, diaphragm) match the illumination of the scene. The histogram can be modified through equalization, stretching or shape modification.

5.1.2 Spatial modification

Spatial methods use digital filters called local operators for picture conversion, including low-pass filters, high-pass filters and median filters.

5.1.3 Frequency modification

In the frequency modification methods, all conversions are performed in the domain of brightness function transform, and the final picture is obtained by applying a reverse transform.

5.1.4 Morphological operations

Morphology–based operations prove to be the most important image processing techniques and they have prevalence over the spatial and frequency methods. A specific operation is undertaken only when defined circumstances are fulfilled. Hence, very precise picture processing is feasible. This techniques will be the one selected for this investigation. A better explanation of these techniques is presented on the next section.

5.2 MORPHOLOGICAL OPERATIONS

5.2.1 STRUCTURING ELEMENT

The structuring element is the most fundamental notion in mathematical morphology. Morphological operations apply a structuring element to an input image, moving it over the whole surface of the picture creating an output image of the same size as the input one. In a morphological operation, the value of each pixel in the output image is based on a comparison of the corresponding pixel in the input image with its neighbors. By choosing the size and shape of the neighborhood, you can construct a morphological operation that is sensitive to specific shapes in the input image.

5.2.2 BASIC OPERATIONS

The most basic morphological operations are dilation and erosion. Dilation adds pixels to the boundaries of objects in an image, while erosion removes pixels on object boundaries. The number of pixels added or removed from the objects in an image depends on the size and shape of the structuring element used to process the image. In the morphological dilation and erosion operations, the state of any given pixel in the output image is determined by applying a rule to the corresponding pixel and its neighbors in the input image. This rule used to process the pixels defines the operation as dilation or erosion. These rules are:

- Dilation: The value of the output pixel is the maximum value of all the pixels in the input pixel's neighborhood. In a binary image, if any of the pixels is set to the value of 1, the output pixel is set to 1.
- Erosion: The value of the output pixel is the minimum value of all the pixels in the input pixel's neighborhood. In a binary image, if any of the pixels is set to the value of 0, the output pixel is set to 0.

Morphological erosion and dilation can be combined to execute morphological opening and closing operations. The first one consists on an erosion operation followed by a dilation operation while the second one is the opposite. Morphological opening and closing are the two operations preferably used during this research. For example, the morphological opening operation is used to remove small objects from a picture while preserving the shape and size of other objects in the image. Other morphological operations are thickening and cutting or skeletonization and shearing.

5.3 IDENTIFICATION OF COLOURS

One of the most important and at the same time most difficult part of the process is to identify the blue whirls and the red ones. As it was explained before, the injection of two kinds of markers (blue and red) was going to be helpful in order to make the separation of the vortices an easier work. The distance between consecutive vortices of the same color is longer (approximately double) than the separation between consecutive vortices if the picture did not have colorant. Hence, the risk of gluing two vortices during the image processing is way lower when using colorants.

In this project, two sets of 8 pictures were analyzed and each of the sets corresponded to photos taken in intervals of 10 milliseconds. However, in order to show the different approaches made to separate the picture, only one of the pictures is going to be presented here as an example. The chosen picture is the sixth one of the first set of pictures (from now on, the pictures of the first set will be referred as Pictures 1 to 8 and the pictures from the second set as Pictures 9 to 16). Picture 6 (Figure 5.1) was selected because it is representative of the style of pictures that are found in the two sets analyzed. The size of Picture 6 is 121 pixels long and 364 pixels wide and, as well as the rest of the photos, it was stored in memory as a bitmap ('bmp') file. As it is a RGB (Red, Green, Blue) image, three different components could be easily identified. Each of the three image components has an 8-bit value (0-255) assigned for each of the pixels of the picture.

Figure 5.1 – Picture 6 as an RGB image

As a first visual approach, it is straightforward to identify a small red whirl and a bigger blue whirl on the left hand side of Picture 6. Just to the right of these first two whirls, another red and blue whirl can be guessed. On the right third of the picture the visual identification of the whirls becomes very complicated. The limited quality of the picture, along with other elements such as the nature of hydrodynamic phenomena and the direct injection tracer method, make the identification of the blue and red whirls on the far side from the bluff body very challenging. Knowing these limitations, it was expected that the image processing of the pictures was going to be much more inaccurate on the second half of the photos that on the first one.

Several techniques were tried in order to obtain good grayscale images where blue whirls and red whirls could be separately identified and processed. Even though the conditions were not the best ones, a pretty acceptable approach was found in order to separate the blue and whirls to be treated separately. Some of the techniques tried are explained now.

5.3.1 RGB MODEL

The first obvious approach to the problem had to be to check if the red and blue colorant were “pure” enough to match with the red and blue components of the original image. In Figures 5.2 to 5.5 the red and blue components of the picture and their histograms are presented. To make it easier to compare, each component figure carries above it the original image so the reader can observe the differences. As it was predictable, this separation is not good enough. In fact, it has a lot of deficiencies that further morphological operations cannot fix. Paradoxically, the grayscale image of the red component seems to fit fairly good with the blue whirls, adding the first red whirl. From these images, it was possible to conclude that the blue dyed fluid marker was not pure blue and that it had also red components. Therefore, this way of trying to separate the image into two grayscale images where the respective whirls can be identified was not feasible

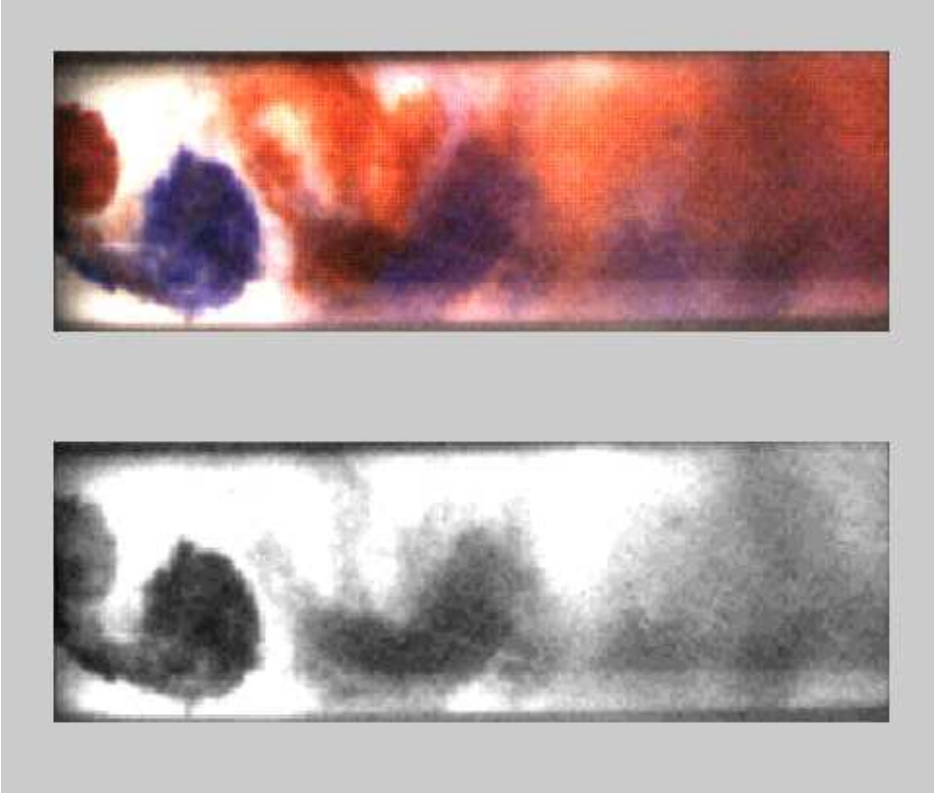

Figure 5.2 – Blue component of the RGB original image

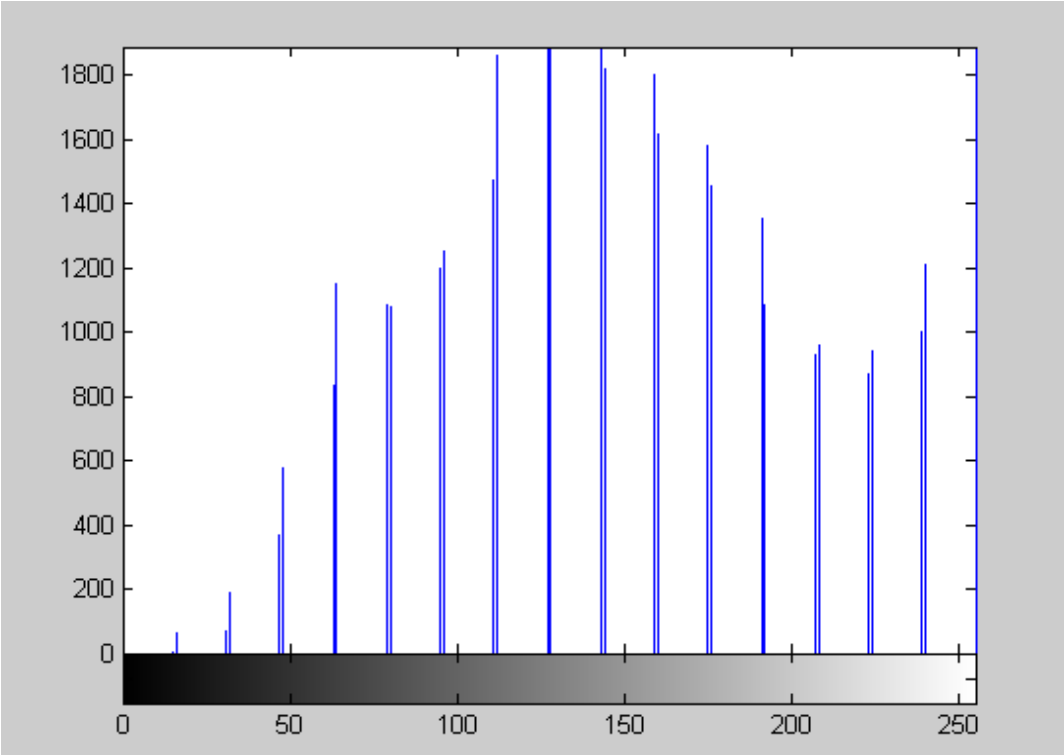

Figure 5.3 – Histogram of the blue component of the RGB original image

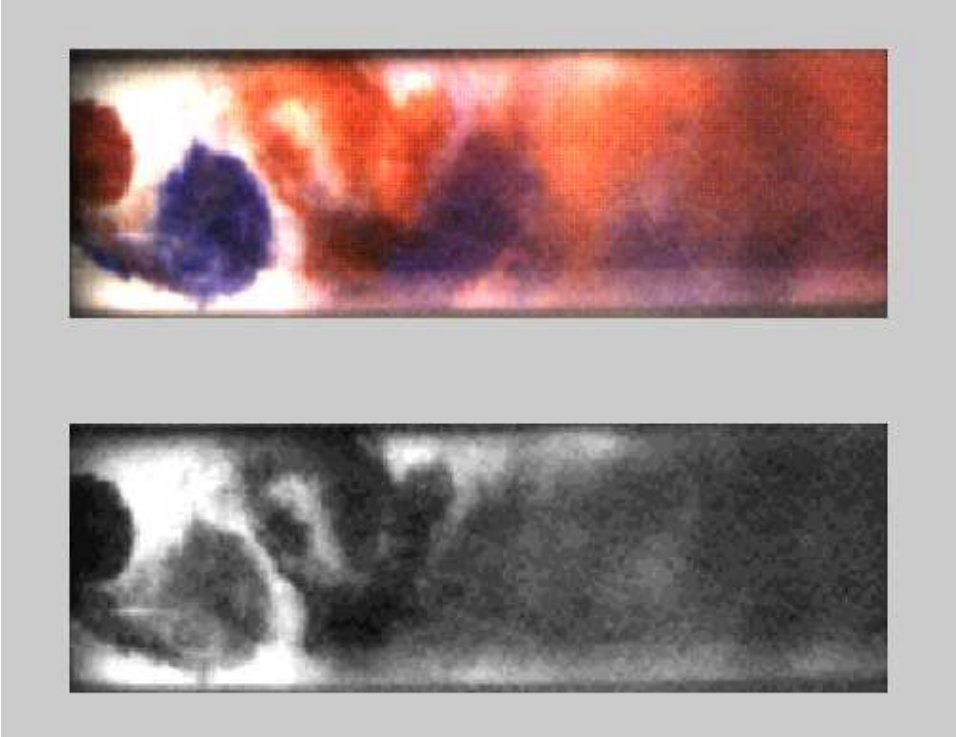

Figure 5.4 – Red component of the RGB original image

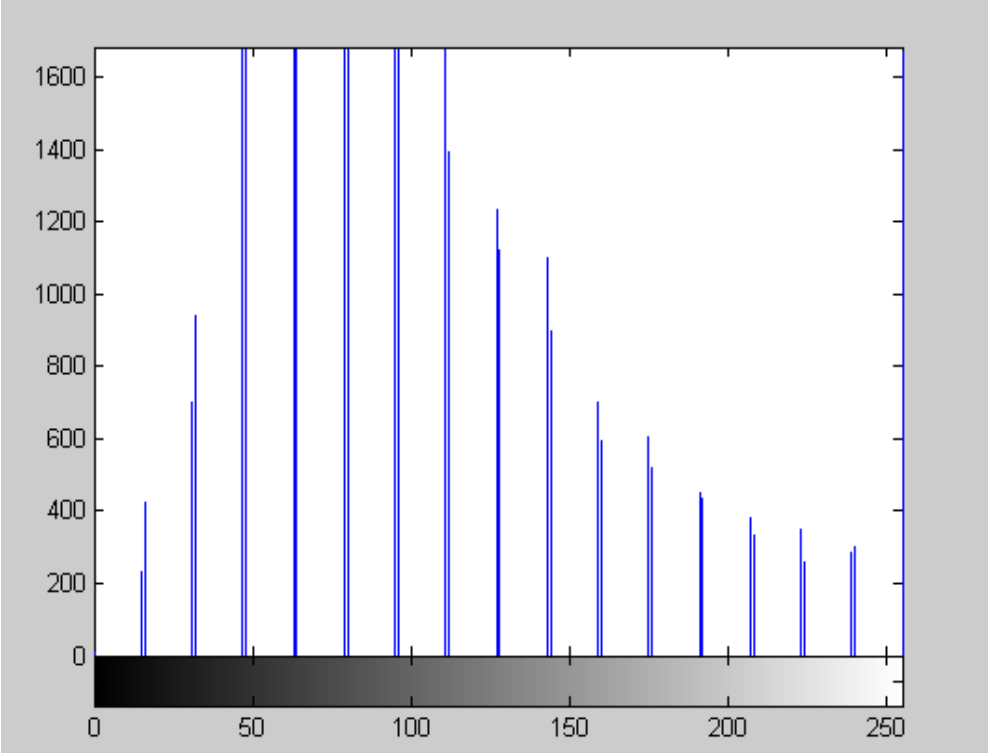

Figure 5.5 - Histogram of the red component of the RGB original image

5.3.2 YQI MODEL

The logical next step was to follow the method used at the mentioned Pankanin paper. Using that method, the RGB image is converted to the YIQ model using a procedure of masks. Although the success using that method seemed obvious in the documentation, it would not work for the set of pictures focus of this study.

Following the procedure, the first step is to apply the luminance mask calculating it by:

$$Y = 0.299R + 0.587G + 0.114B$$

Being R, G and B respectively the red, green and blue components of the original picture's pixels. The determination of the concurrence of vortices is supposed to be easy since the luminance value describes the level of brightness. Applying the luminance mask to the initial Picture 6 (Figure 5.1), the left hand side whirls are well detected. However, as we move to the right, the blurriness of the whirls makes it impossible for the mask to separate the actual whirl from the background.

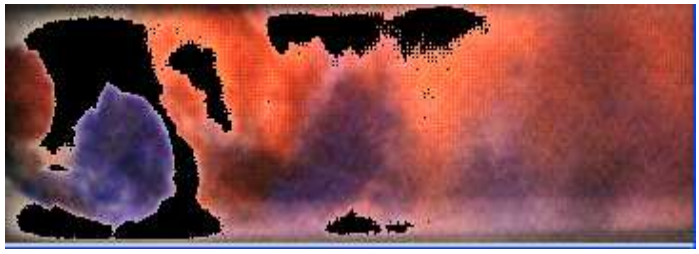

Figure 5.6 – Picture 6 after applying the luminance mask

The next two steps (Figure 5.7 and Figure 5.8) were made taking account of the sake of color (Q) and the sake of color saturation (I). The calculations where made using the formulas of the YQI model:

$$Q = 0.48 (R – Y) + 0.4 (B – Y)$$

$$I = 0.74 (R – Y) – 0.27 (B – Y)$$

Figure 5.7 – Picture 6 after applying the second step

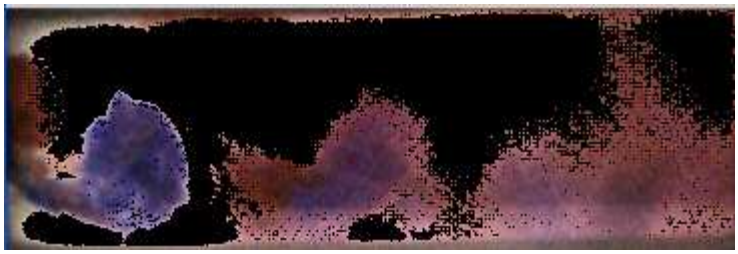

Figure 5.8 – Picture 6 after applying the third step

Unfortunately for this research, the appliance of the last two steps was not helpful. The original intention of those steps was to make it easier to identify the whirls and then separate them into blue and red whirls. Instead, most of the red whirls from the original picture are gone making it impossible to process them and get the desired results.

5.3.3 YUV MODEL

The third tried option was to convert the picture to the YUV model and check if any of the grayscale chrominance components was good enough to separate the whirls of each color. The YUV model divides the picture between a luminance component (Y) and two chrominance components (U and V). The luminance component is calculated using the same formula of the previous YQI case, while the other two components are calculated as:

$$U = B - Y$$

$$V = R - Y$$

Once Picture 6 was transformed into the desired YUV model (Figure 5.9), it was possible to see that a separation of the red and blue vortices was going to be a tough task. In fact, from the results it was going to be observed that this method was not going to work.

Figure 5.9 – Picture 6 transformed to the YUV components

Taking into account the data obtained in the previous YQI attempt, the luminance results were the expected. In (Figure 5.10) the bigger intensity of the whirls comparing to the background (especially on the left side of the picture) makes the whirls distinguishable.

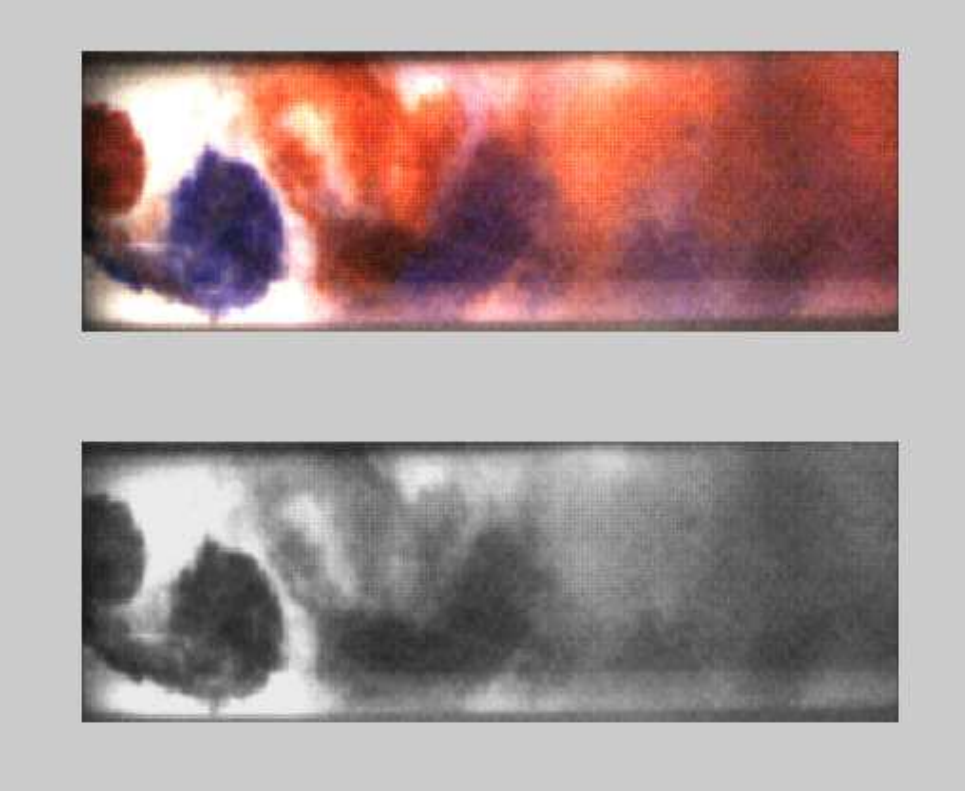

Figure 5.10 – Y component of Picture 6

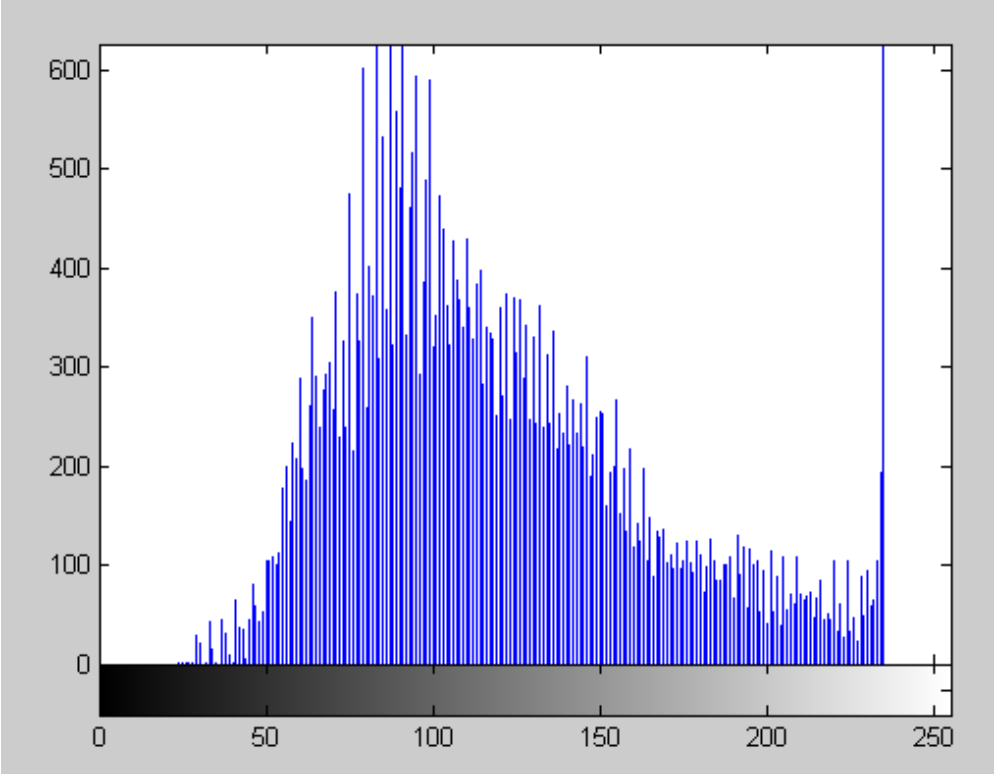

Figure 5.11 – Histogram of the Y component of Picture 6

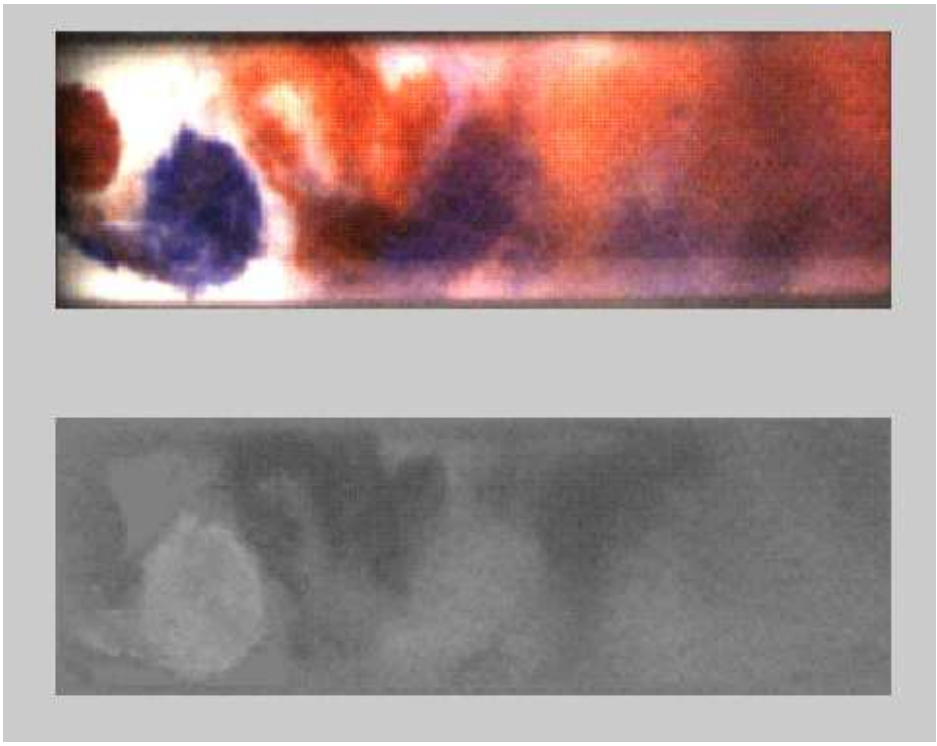

Figure 5.12 - U component of Picture 6

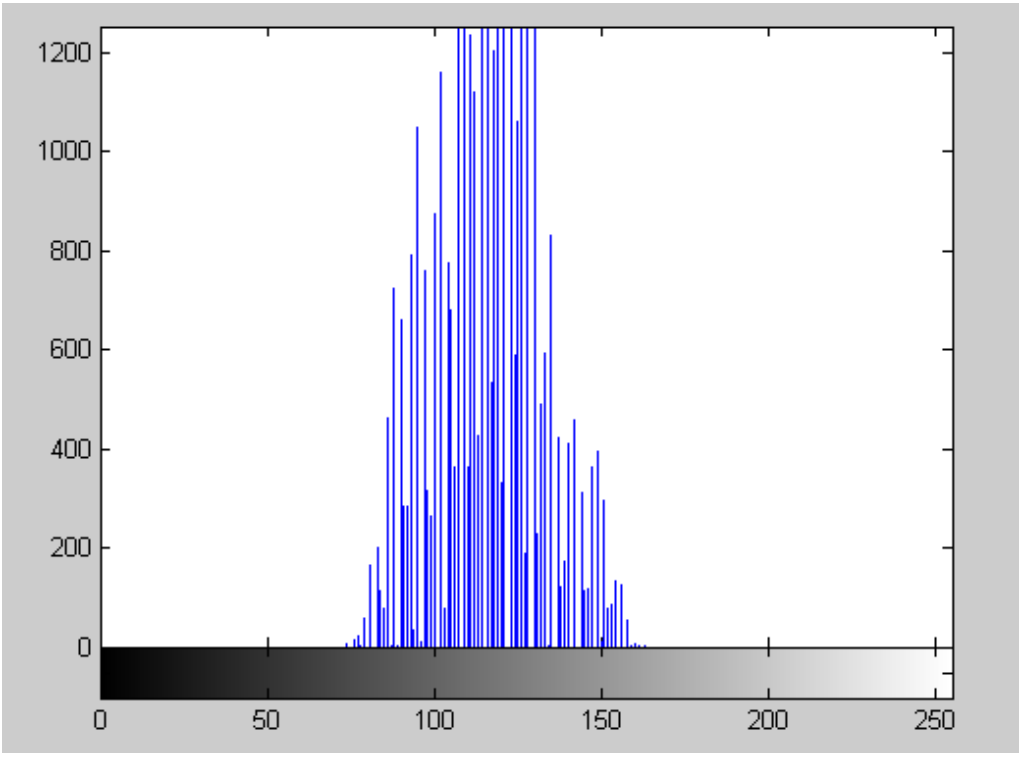

Figure 5.13 - Histogram of the U component of Picture 6

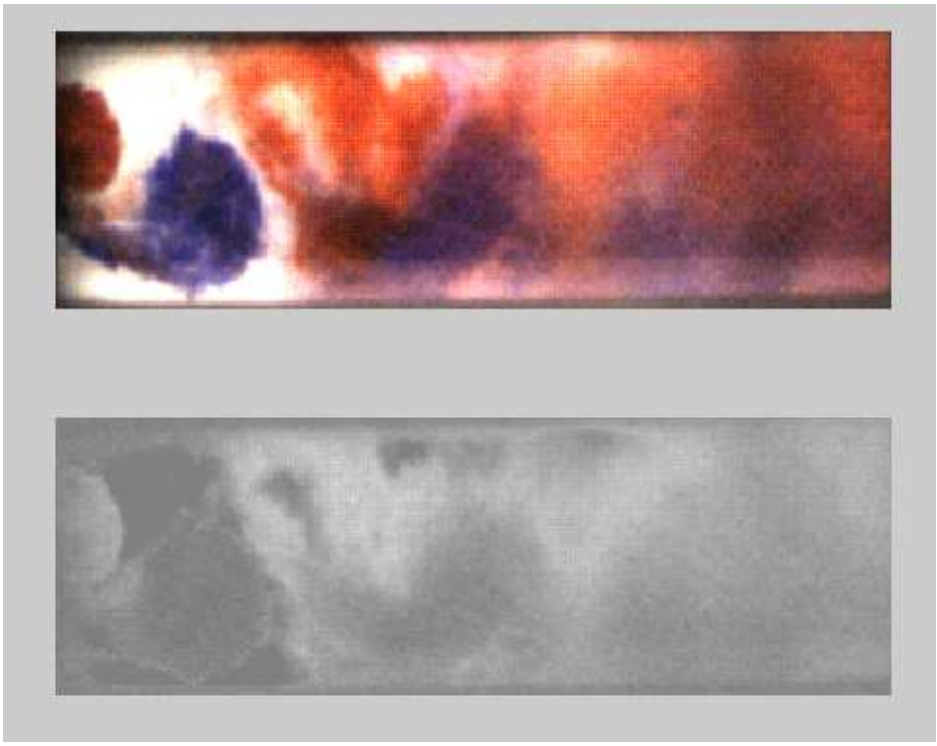

Figure 5.14 - V component of Picture 6

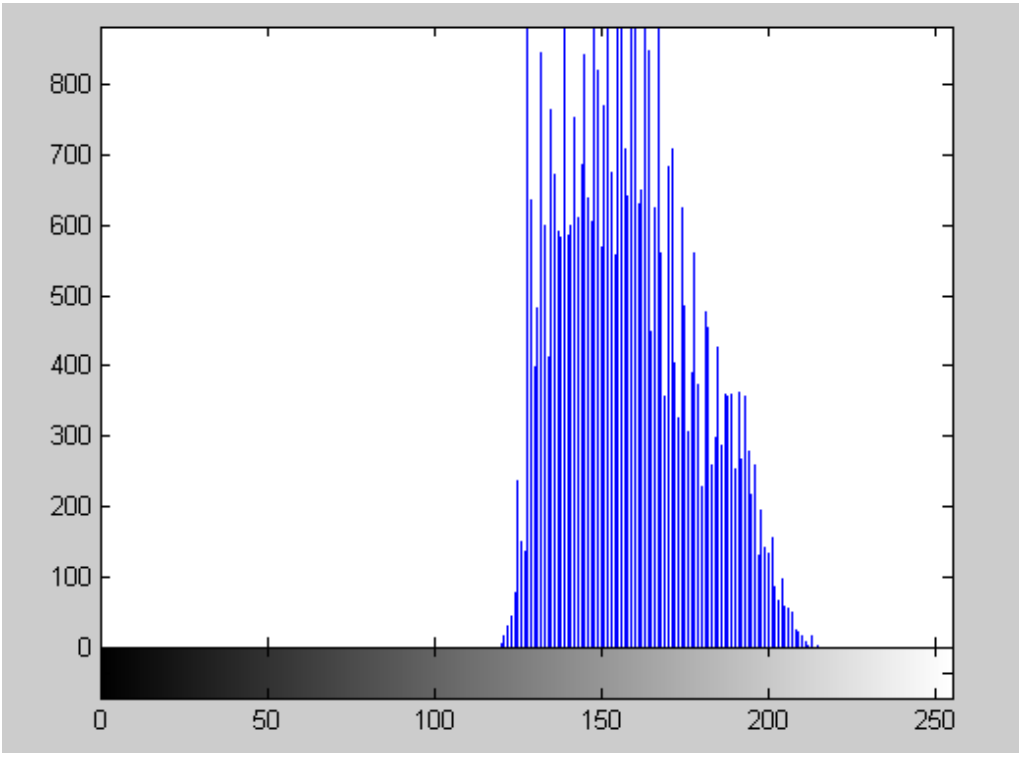

Figure 5.15 - Histogram of the V component of Picture 6

However, there is no information obtainable from the two chrominance components (Figures 5.12 and 5.14). The narrowness of their histograms made these pictures very difficult to be transformed into a reliable black and white picture and therefore no morphological operations could be done.

5.3.4 HSV MODEL

The final and best approach to the problem was transforming the image into the HSV components, which stands for Hue, Saturation and Value. The first positive result comes with the Figure 6 transformation to the HSV components. In Figure 5.16 it is appreciated how the red and blue whirls are distinguishable and they have different hues and intensities. Therefore, further work on the separate H, S and V components could make it possible to obtain independent grayscale images for red and blue vortices.

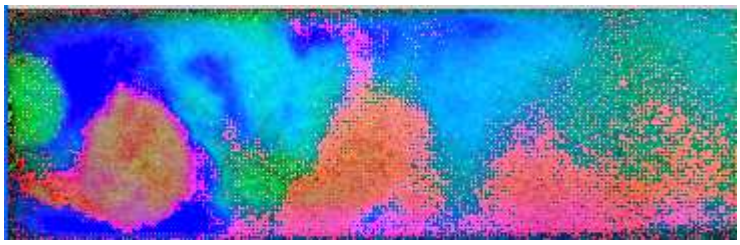

Figure 5.16 – Picture 6 transformed to the HSV components

The first step then was to analyze the Hue component and check if the blue and red whirls had indeed different values. It can be seen in Figure 5.17 how the results were even better than expected. The red whirls, as well as the background, have a low small numerical value of hue so the blue whirls are totally visible. The histogram (Figure 5.18) shows a very big distance between the background plus the “red” pixels, and the “blue” pixels, making it very easy to transform the H component into a valid black and white picture.

Identifying the red vortices was not that straightforward, but it was still feasible. Taking a look at the saturation (S) component of the image (Figure 5.19), it is observable that the red vortices are well distinguished from the background. However, blue vortices are still included in the whiter area. To solve this problem, a very simple solution is proposed: simply subtract the H component (blue whirls) from the S component (blue + red whirls). Figure 5.21 shows the result of this S-H component and the improvements can be easily observed. As it was predicted since the beginning of the investigation, the right hand side of the picture is very difficult to analyze and the results are not perfect, but this grayscale image is the best approach reachable using the methods discussed in this section.

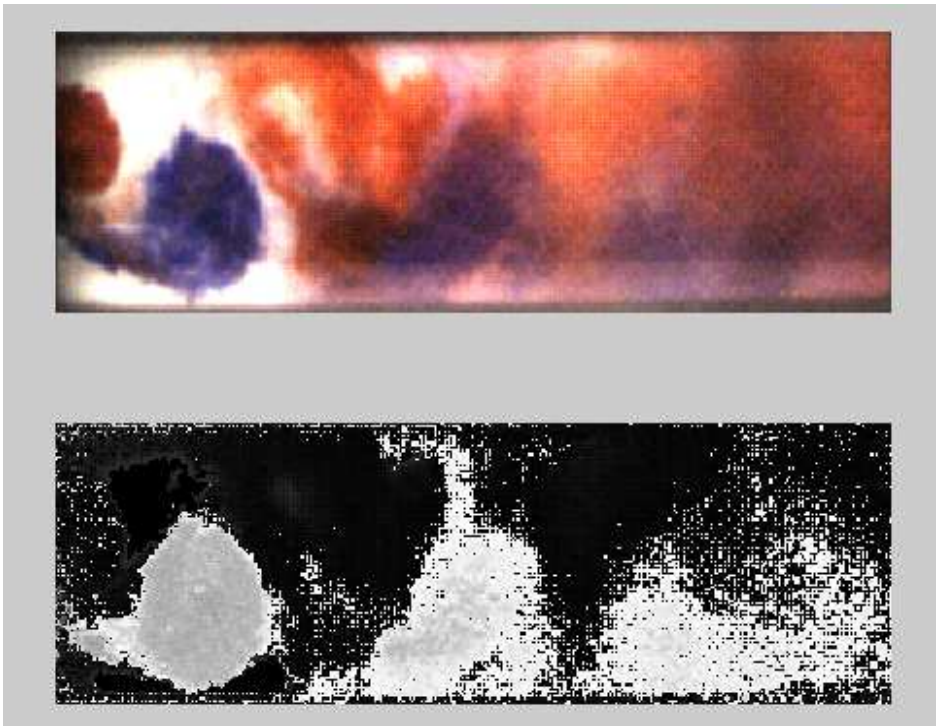

Figure 5.17 – H component of Picture 6

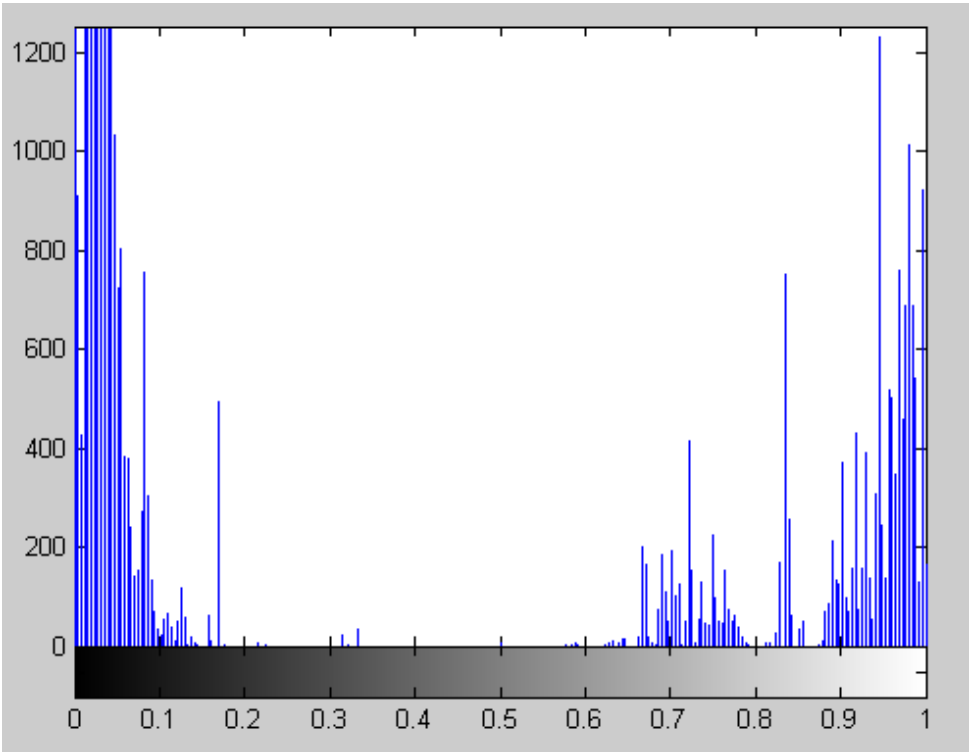

Figure 5.18 – Histogram of the H component of Picture 6

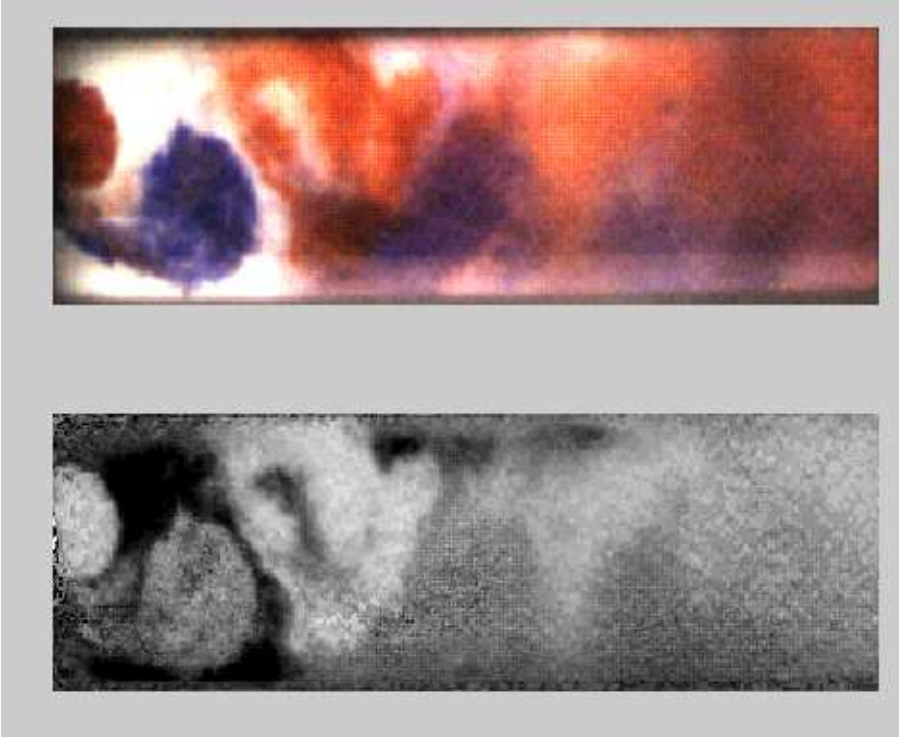

Figure 5.19 - S component of Picture 6

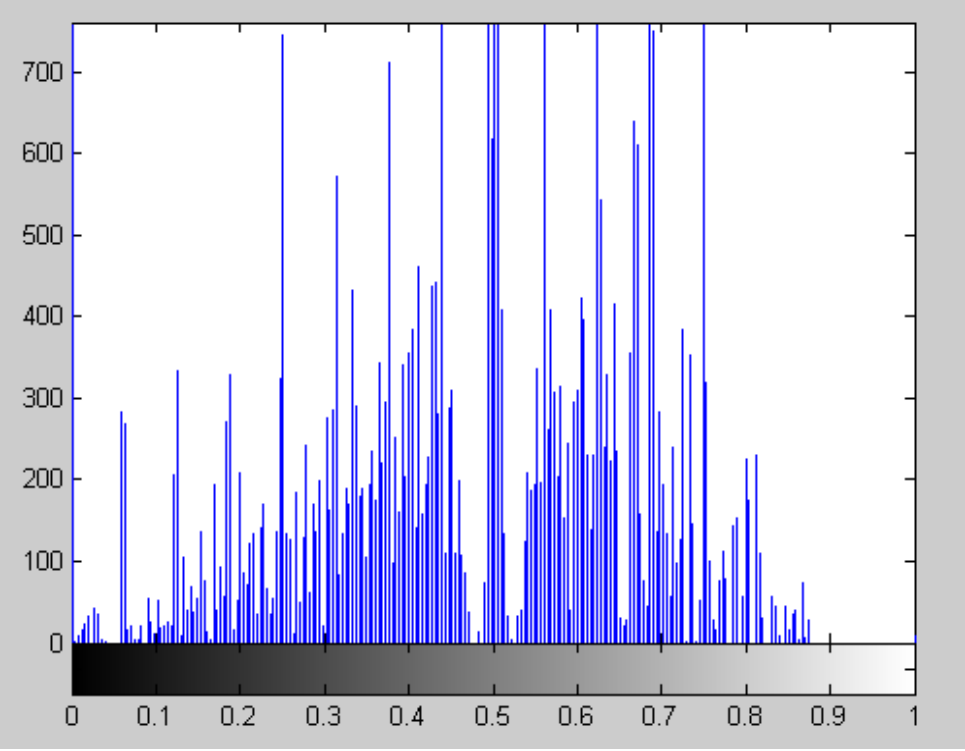

Figure 5.20 – Histogram of the S component of Picture 6

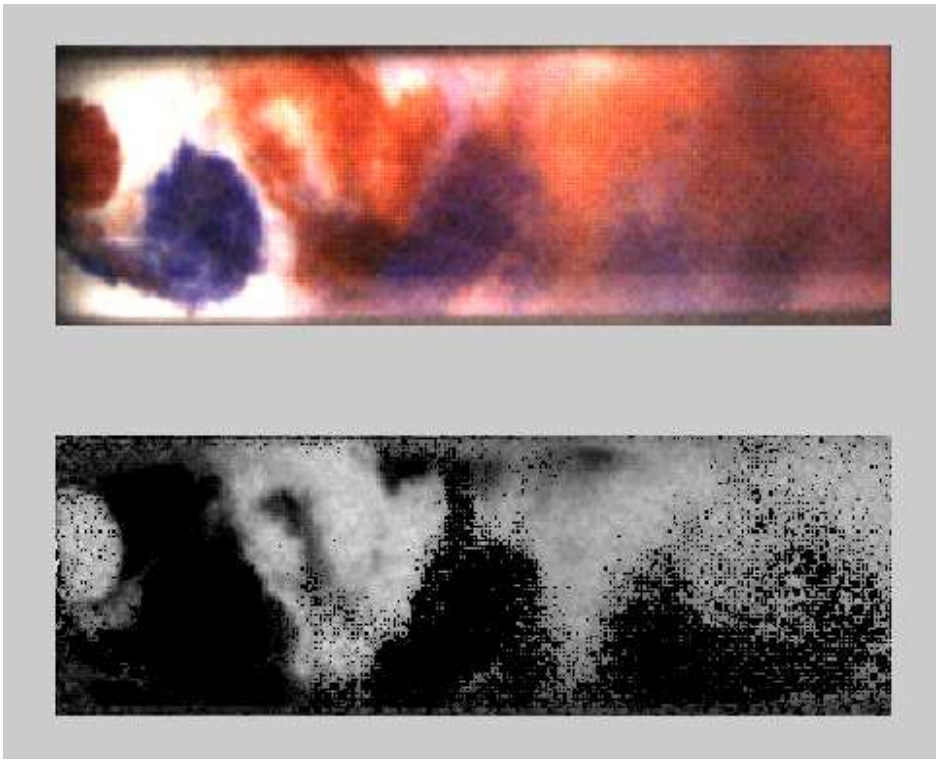

Figure 5.21 – S–H component of Picture 6

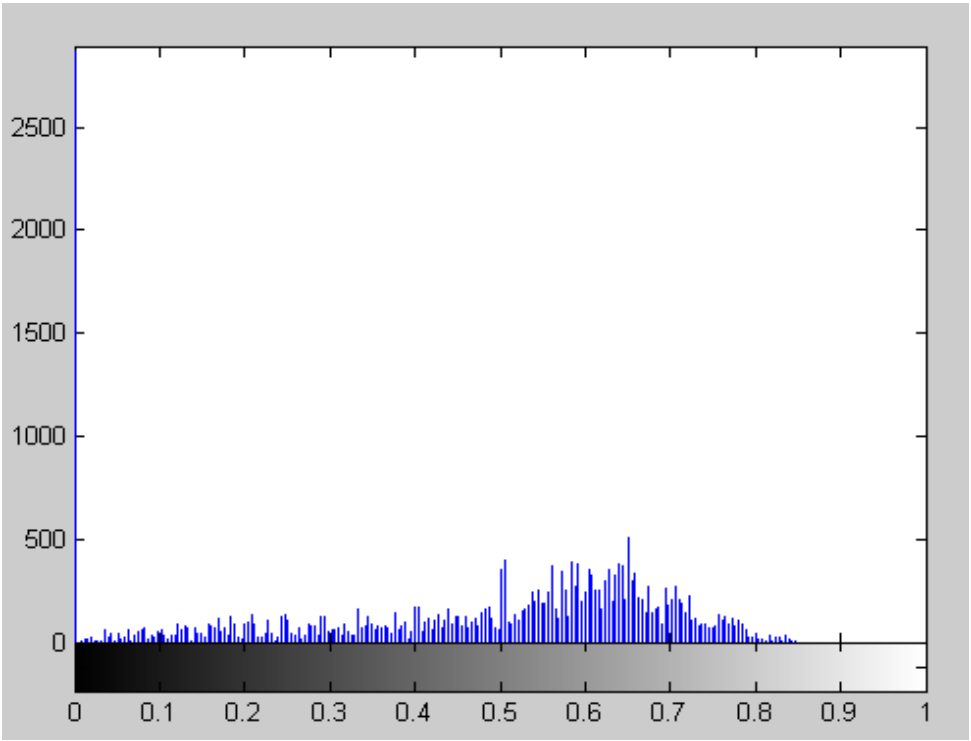

Figure 5.22 – Histogram of the S–H component of Picture 6

The method was presented using Picture 6 as an example but it could be easily applied to the rest of the pictures of both sets. The final results are presented on Figures 5.23-5.26 for the blue whirls and on Figures 5.27-5-30 for the red whirls.

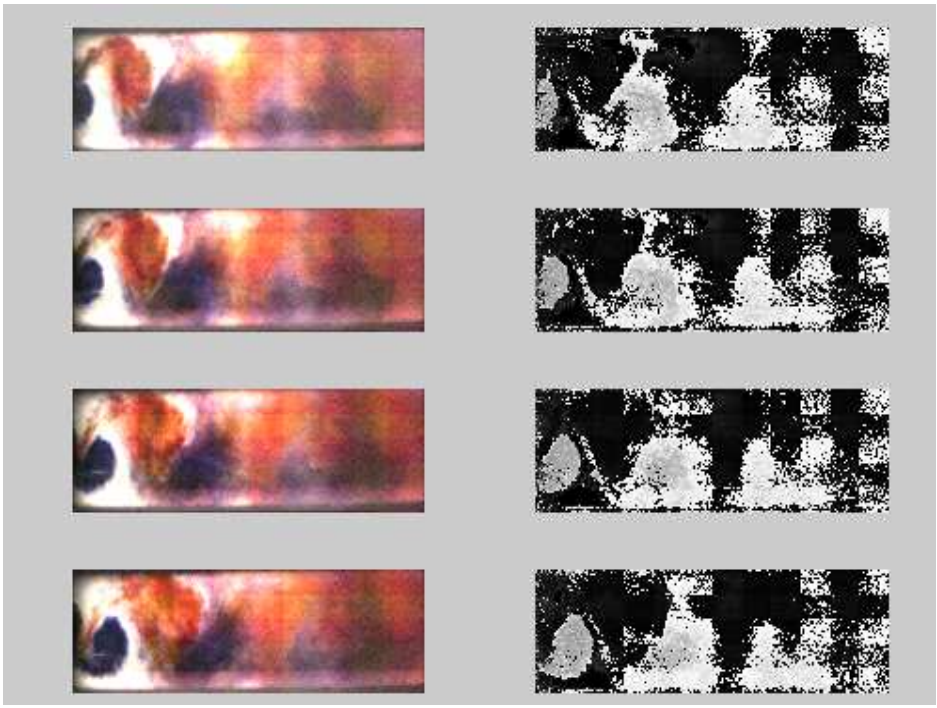

Figure 5.23 – Blue whirls of Pictures 1-4

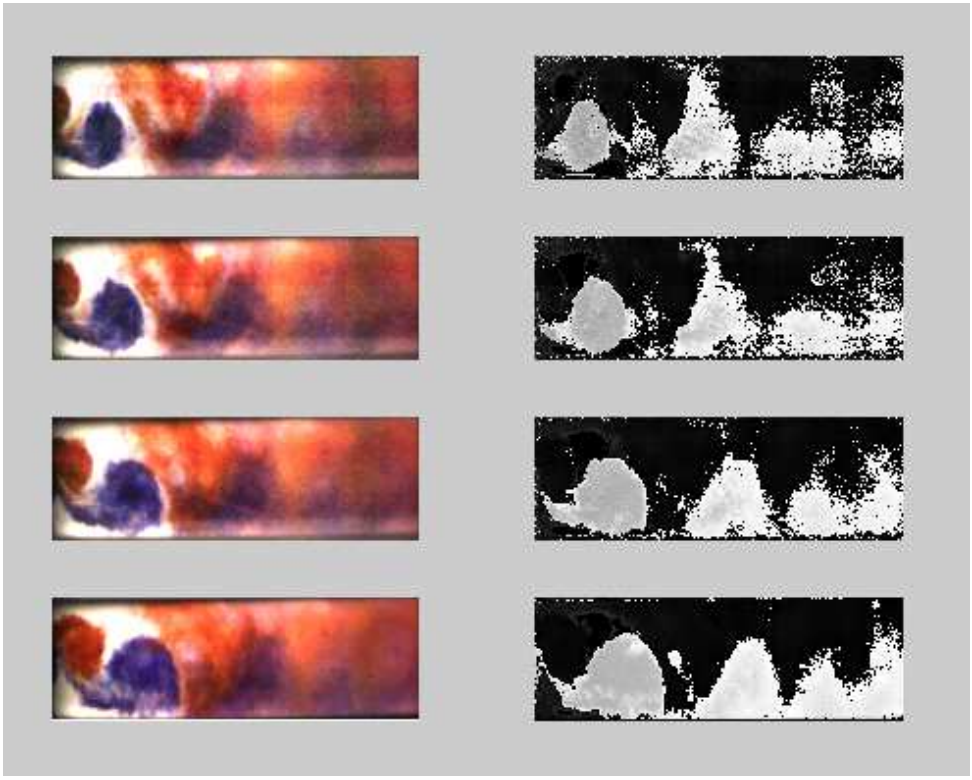

Figure 5.24 – Blue whirls of Pictures 5-8

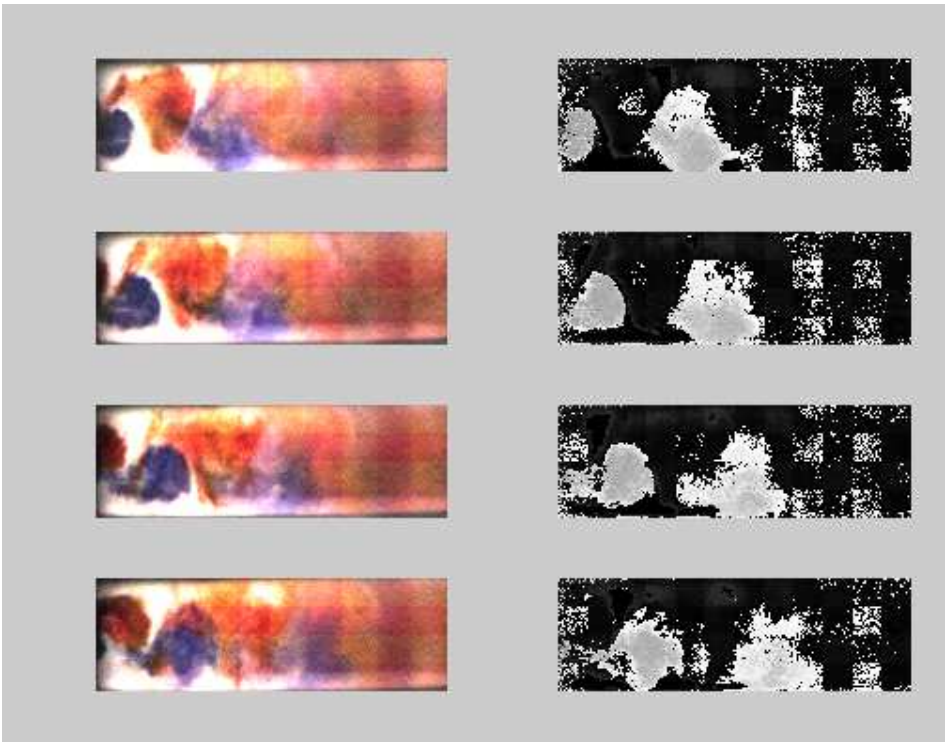

Figure 5.25 – Blue whirls of Pictures 9-12

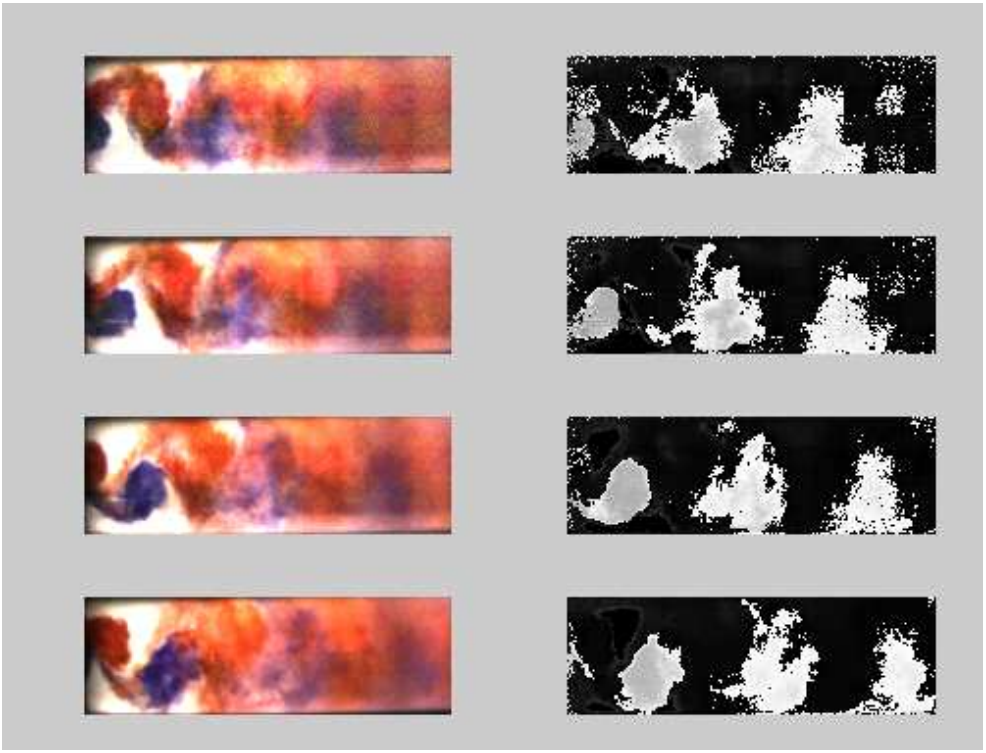

Figure 5.26 - Blue whirls of Pictures 13-16

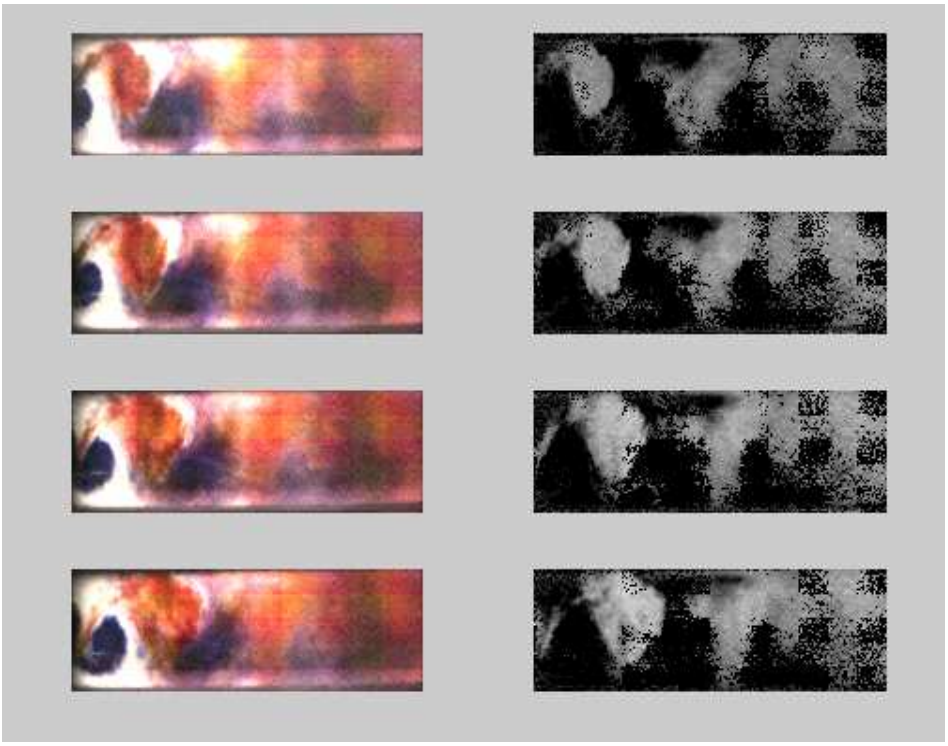

Figure 5.27 - Red whirls of Pictures 1-4

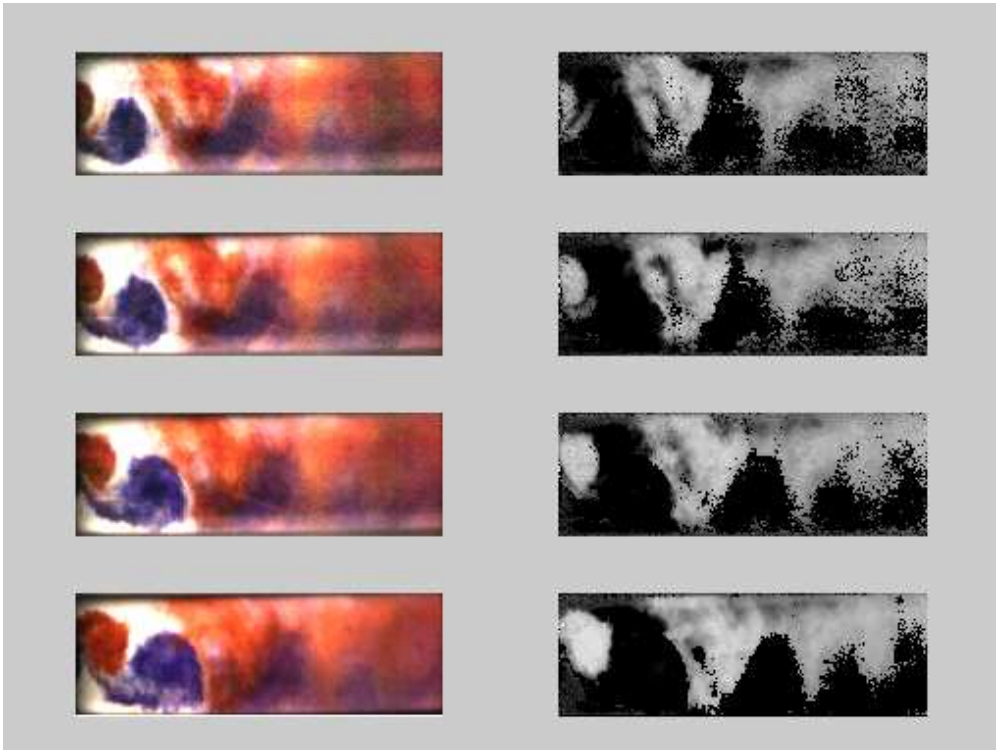

Figure 5.28 - Red whirls of Pictures 5-8

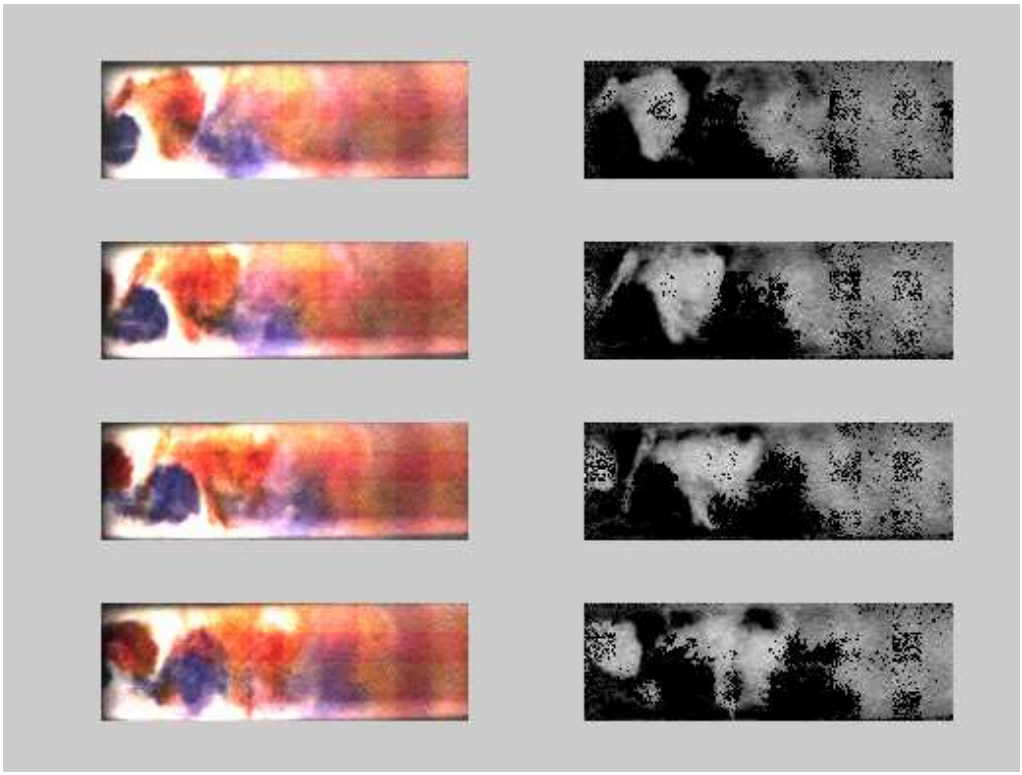

Figure 5.29 - Red whirls of Pictures 9-12

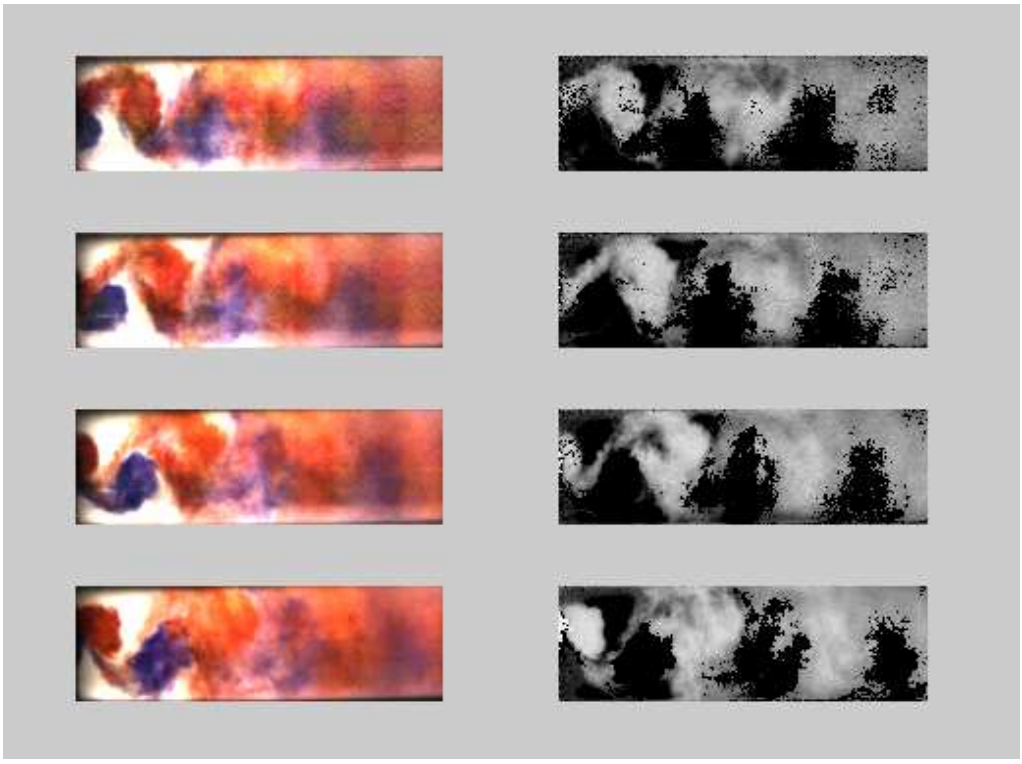

Figure 5.30 - Red whirls of Pictures 13-16

5.4 SEPARATION OF VORTICES

Once grayscale one-dimensional images are obtained for both colors and both sets of pictures, morphological operations can be executed. But in order to make this kind of operations, the pictures need to be previously transformed from grayscale to black and white. The histograms on Figures 5.20 and 5.22 show that the values assigned to the pixels of the new images vary from 0 (black) to 1 (white). This means that in order to convert this image into a black and white one, a threshold value has to be chosen in the [0,1] interval so the pixels whose values are higher than the threshold value are converted to white, and the ones whose values are lower are converted to black. The election of this threshold is made using the Otsu's method [9], which chooses the value to minimize the intraclass variance of the black and white pixels.

The result of the black and white conversion of the two set of pictures is presented on Figures 5.30-5.37 compared with the grayscale images. Otsu's method worked perfectly on the selection of the threshold and the black background was distinguished from the whirls that were converted to white.

After the black and white pictures were obtained, it was time to start going towards the main goal, which was identifying and separating all the vortices. For that, the following actions were required:

- Make the form of the whirls smoother
- Fill the holes inside the whirls
- Delete all the removable small parts outside the whirls

In order to achieve these objectives, morphological operations are required. But once these actions are successfully finished, the whirls could be easily separated and processed. Hence, this is the most important step of the process, being critical to choose the right operations and the right parameters at the right time. The selection of these parameters was a long and slow process, but fairly successful results were found. It has to be pointed out that the selection of the operations and its parameters was specific for the two set of pictures used during this investigation. A different set of pictures with different features such as color, quality or resolution, would probably need a different approach.

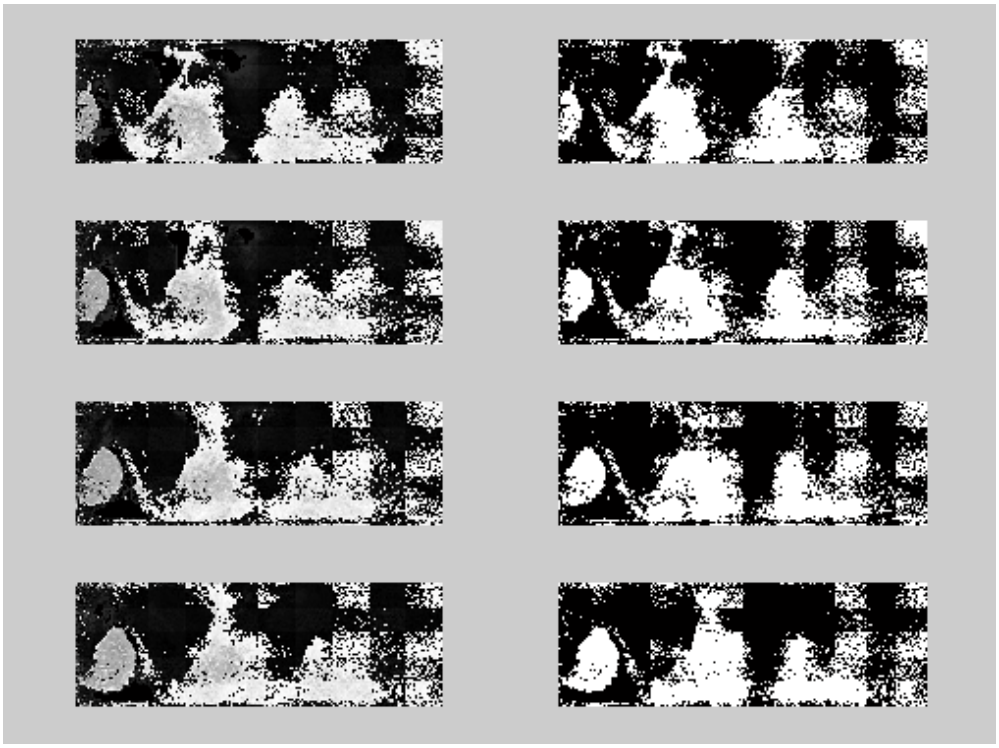

Figure 5.31 – Black and white conversion of the blue whirls of Pictures 1-4

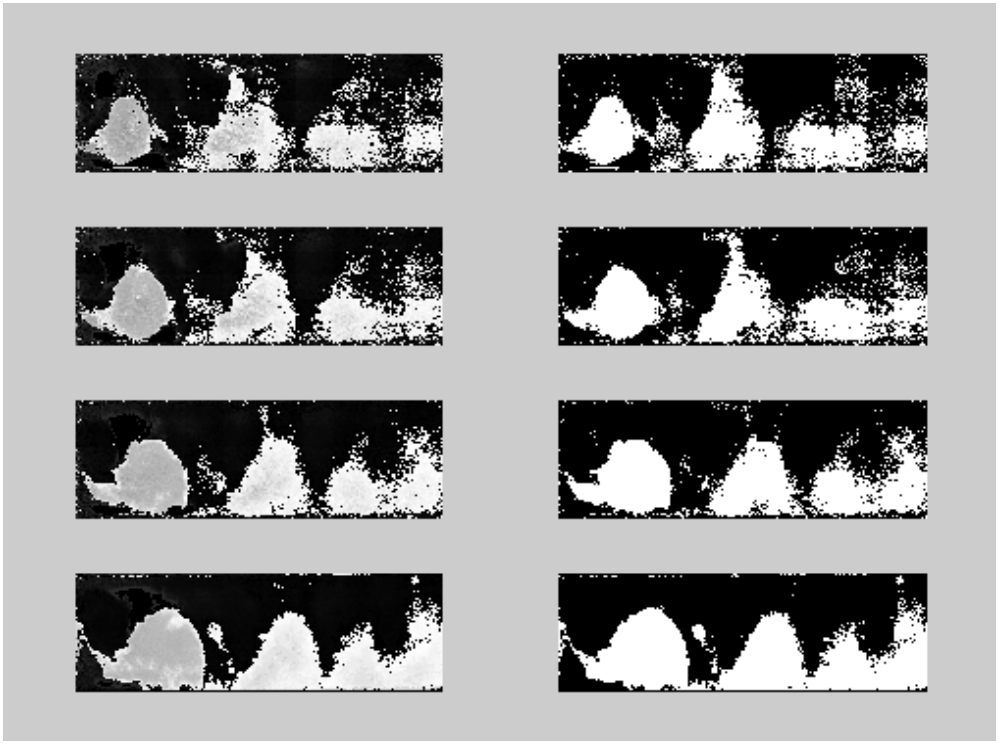

Figure 5.32 - Black and white conversion of the blue whirls of Pictures 5-8

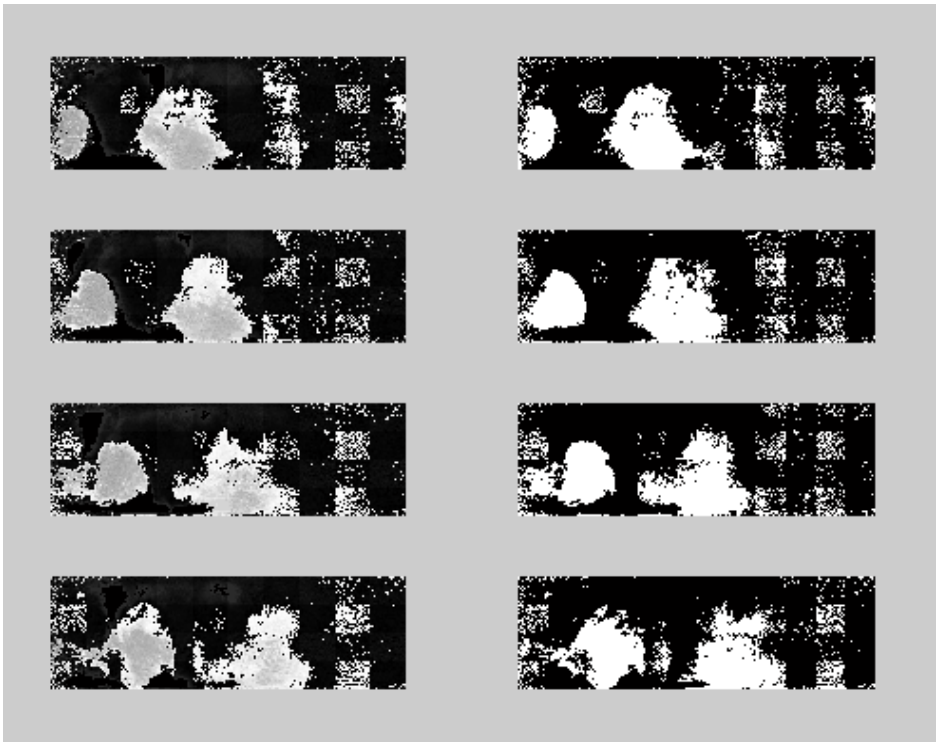

Figure 5.33 - Black and white conversion of the blue whirls of Pictures 9-12

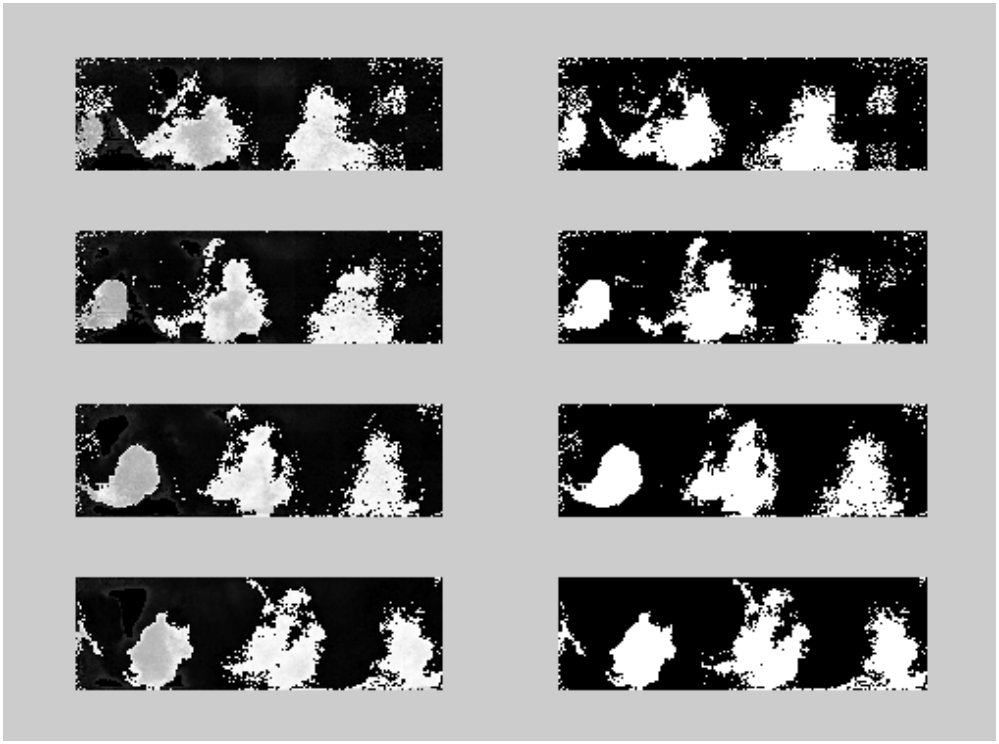

Figure 5.34 - Black and white conversion of the blue whirls of Pictures 13-16

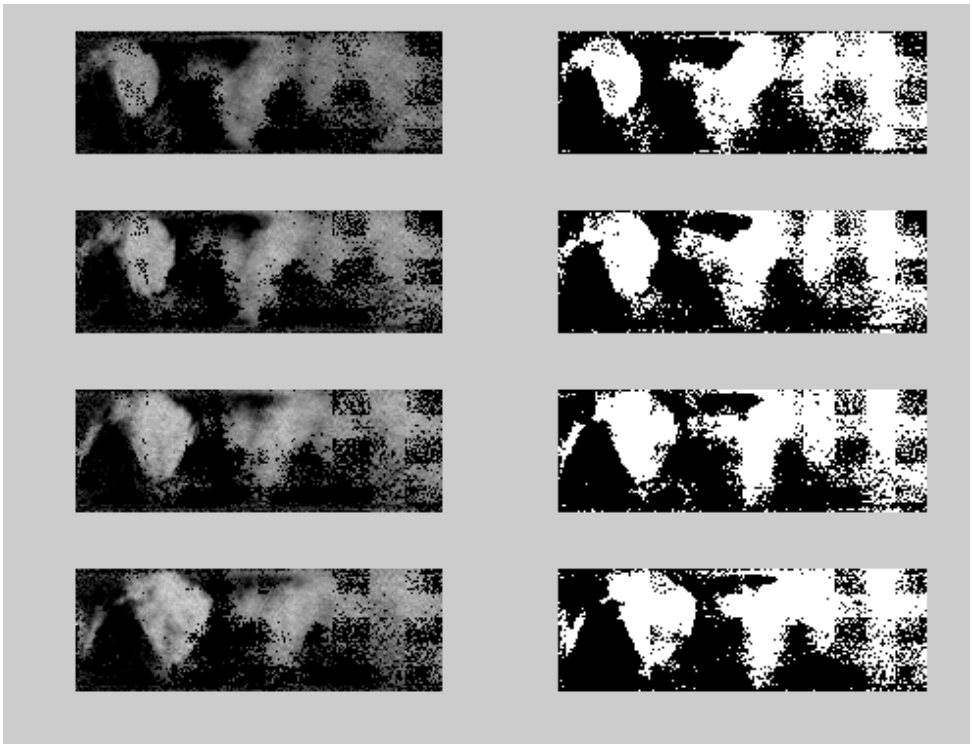

Figure 5.35 – Black and white conversion of the red whirls of Pictures 1-4

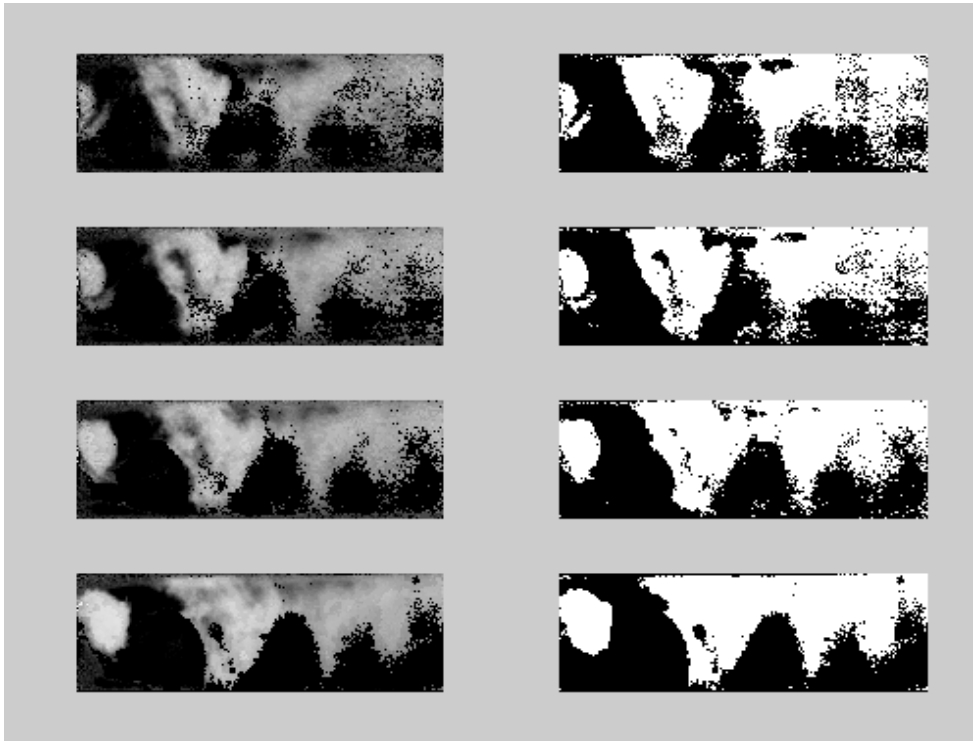

Figure 5.35 - Black and white conversion of the red whirls of Pictures 5-8

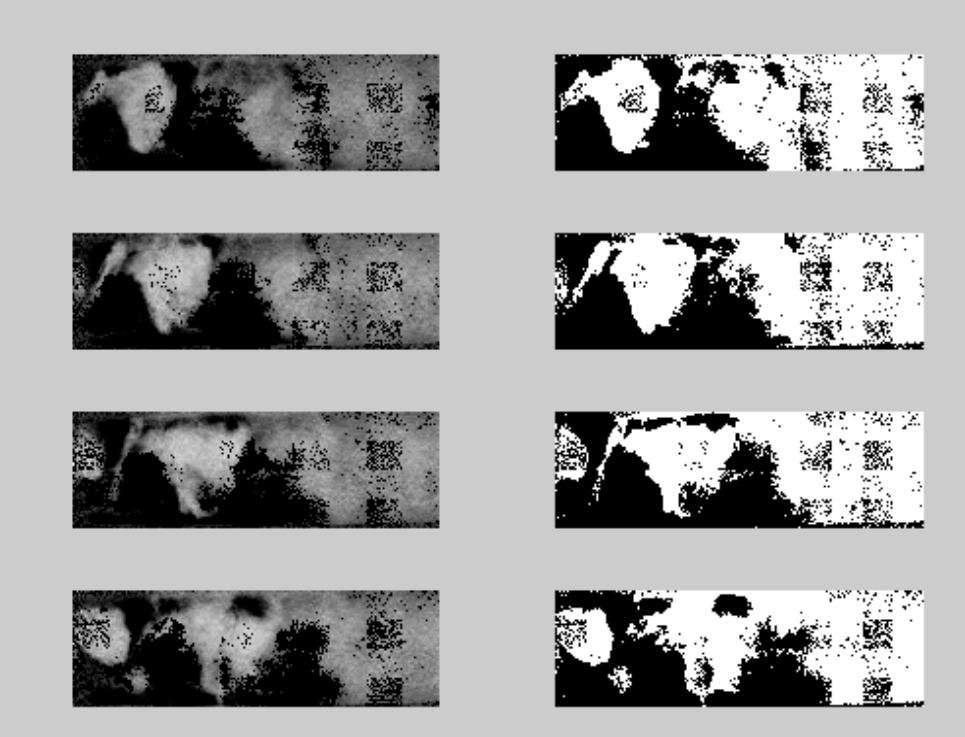

Figure 5.36 - Black and white conversion of the red whirls of Pictures 9-12

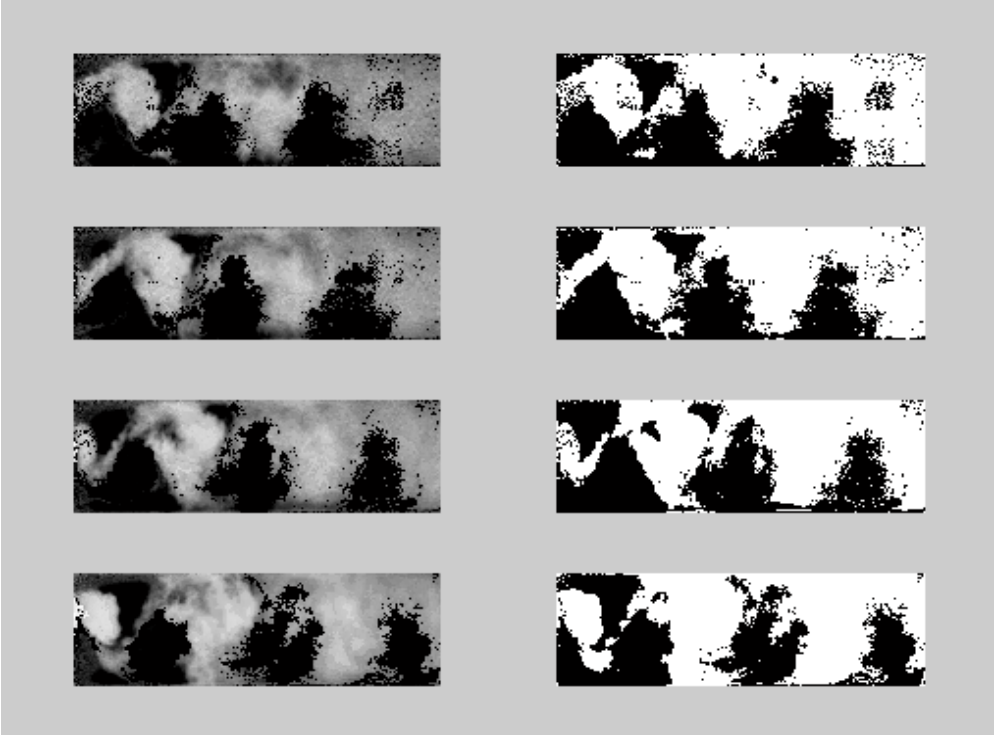

Figure 5.37 - Black and white conversion of the red whirls of Pictures 13-16

Several conclusions were obtained from this process:

- The steps to follow in order to obtain good results are: perform a morphological opening and closing, fill the holes inside the whirls with a specific function, perform an aggressive morphological opening, delete elements whose area is smaller than desired.
- The different characteristics of the pictures and the different form and size of the whirls require a different analysis. Therefore, the parameters used in the morphological operations such as the size of the structuring elements have to be different when analyzing the blue whirls and the red ones.
- The closest part to the bluff body (the left hand side) has better quality than the furthest part so different parameters might be used in order to analyzed both parts. Even though in the pictures of the blue whirls this is not really necessary, it is critical to perform this on the red whirl pictures in order to obtain something satisfactory.

After all the process, Table 5.1 shows the final operations and its parameters selected. Note that the first left quarter of the red pictures were analyzed separately from the rest of the picture:

		Opening	Closing	Opening	Delete area
Blue		SE = 4	SE = 4	SE = 9	< 400
Red	**1st quarter**	SE = 3	SE =3	SE = 6	< 500
	rest	SE = 5	SE = 5	SE = 10	

Table 5.1 – Final morphological operations and parameters selected

Finally, after applying these operations to the pictures presented on Figures 5.30-5.37, the results can be observed on Figures 5.38-5.41.

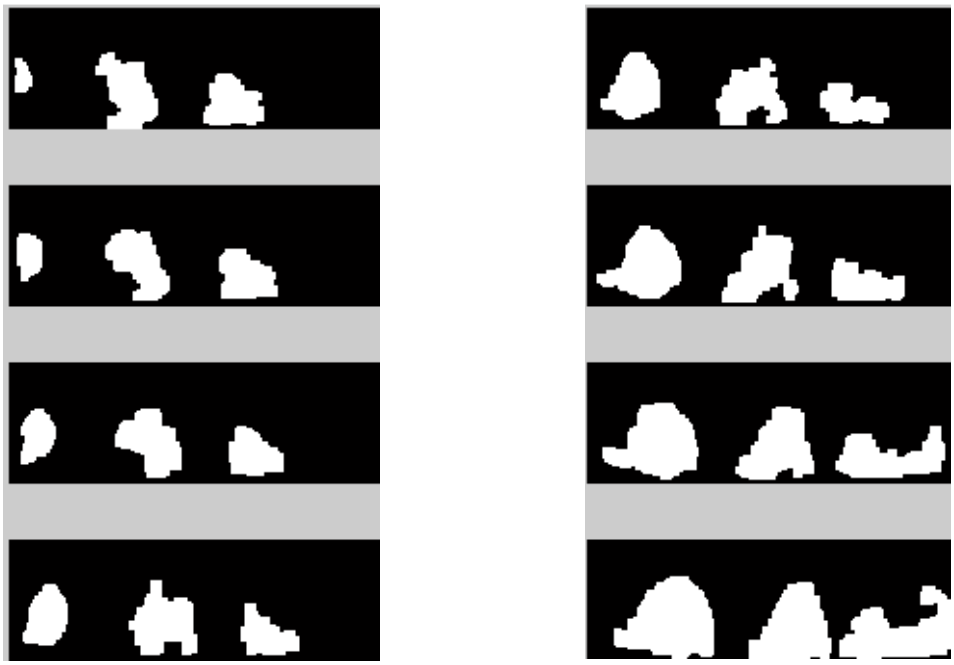

Figure 5.38 – Post-processed black and white blue whirls for Pictures 1-8

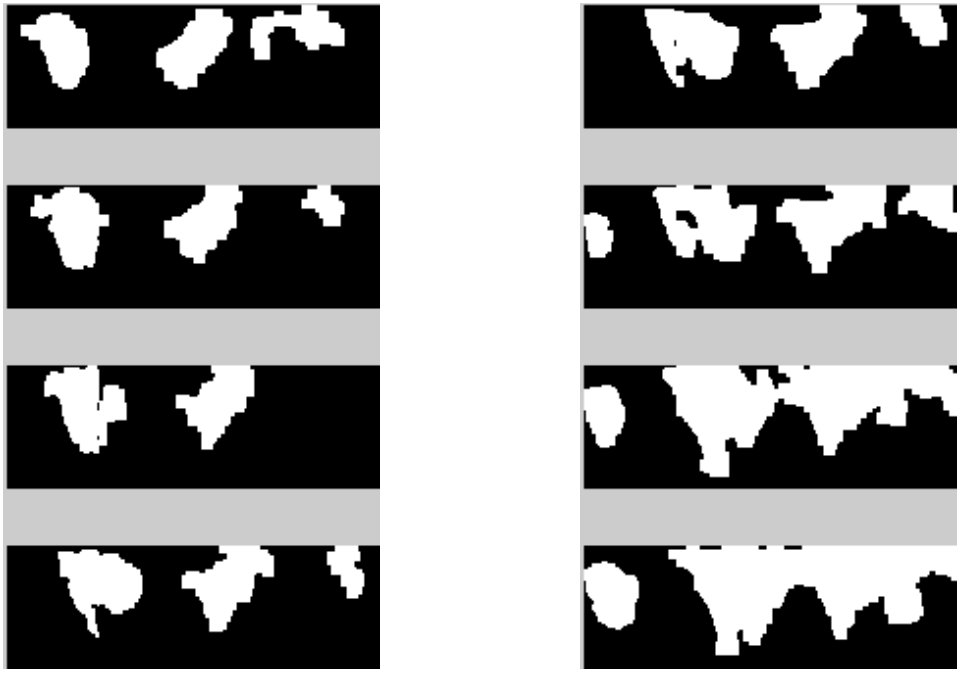

Figure 5.39 - Post-processed black and white red whirls for Pictures 1-8

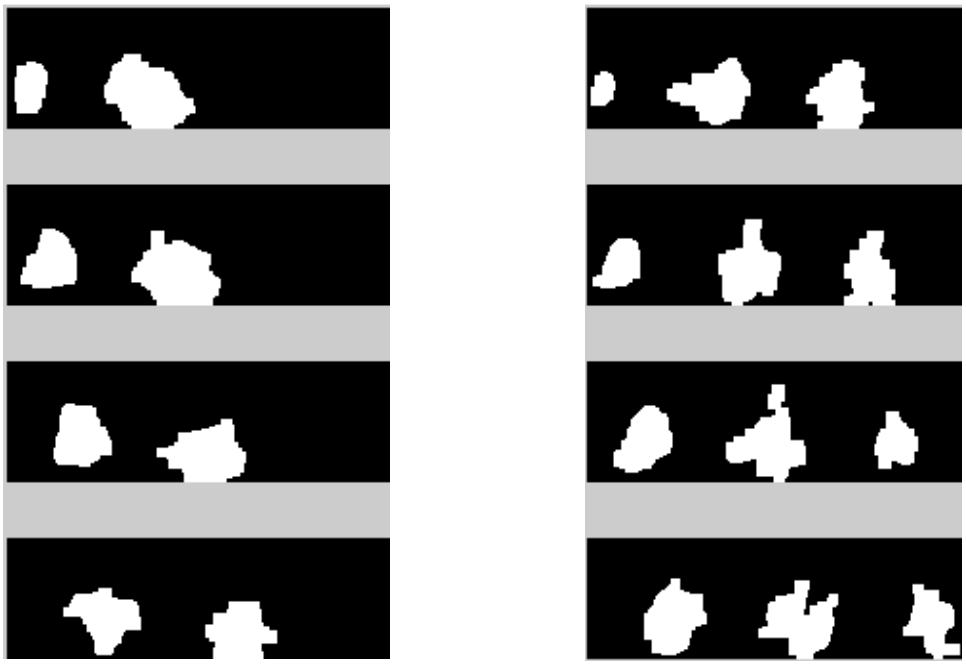

Figure 5.40 - Post-processed black and white blue whirls for Pictures 9-16

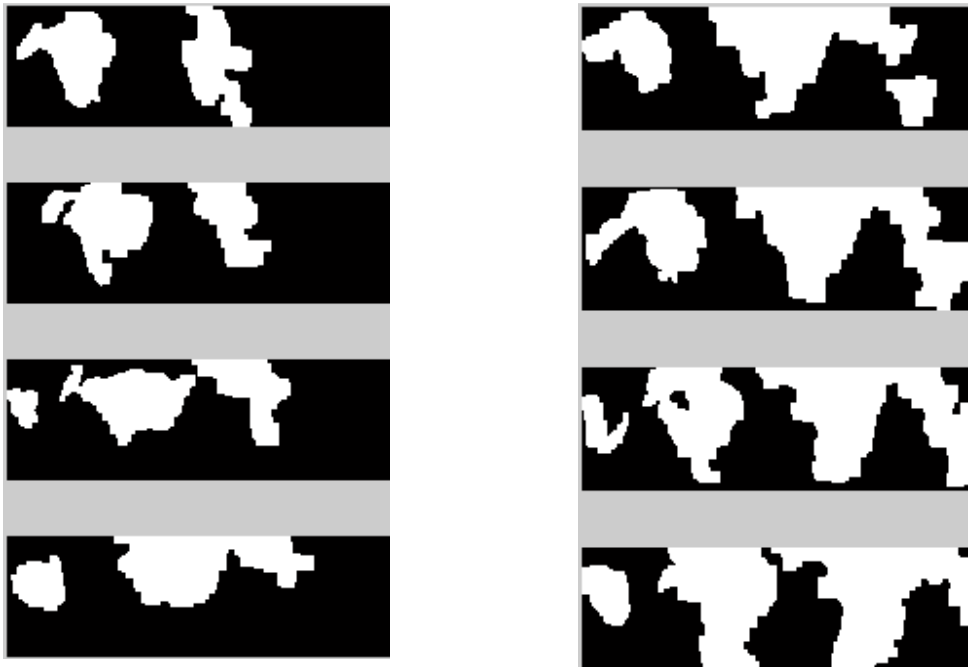

Figure 5.41 - Post-processed black and white red whirls for Pictures 9-16

It is noticeable that in a few pictures the separation was not perfect. This phenomenon is especially dangerous on the right part of the pictures where the quality is not as good as desired. This was the time when the programmer's ability was needed in order to fix those problems. In this specific case for these sets of pictures, some functions were performed so when a suspect extremely wide whirl is found, it is analyzed as there was more than one whirl glued together.

Finally, before moving forward to the next step, the start and end coordinates of the different whirls were obtained so the vortices can be processed separately and the center of gravity of each of them can be calculated.

5.5 CENTER OF GRAVITY

The calculation of the center of gravity is the final step needed in order to obtain and analyze the results this investigation was looking for. In the algorithm previously presented to the author, a very simple method was used to calculate the center, but it was believed that it was not good enough.

In this preliminary method, the black and white picture of the whirl was used. First of all, the white pixels that were the closest and the furthest respectively to the bluff body were selected. The "x" value (the column number if we look at the picture as a matrix of pixels) of the two points were taken and the medium value of them was going to be the column of the future center point. The same thing was made with the "y" values. The white pixel whose value of the "y" coordinate (the row number) was the highest was taken, as well as the pixel whose "y" value was the lowest. Then the medium value of the two was selected as the row of the center point. This method is tested in Figure 5.42 using blue whirls of Picture 6 as an example. It has to be noted that even though the three whirls were presented together, each of them were processed separately using the dividers calculated as explained in the previous section.

Because of the simplicity of the method, it was expected that when the form of the whirl is round or squared (like the first whirl in this case), the method is going to work. However, when the form is not that smooth (like in the third whirl), the method does not give an optimal result. Therefore, another way of calculating the center of gravity had to be designed in order to obtain a better result.

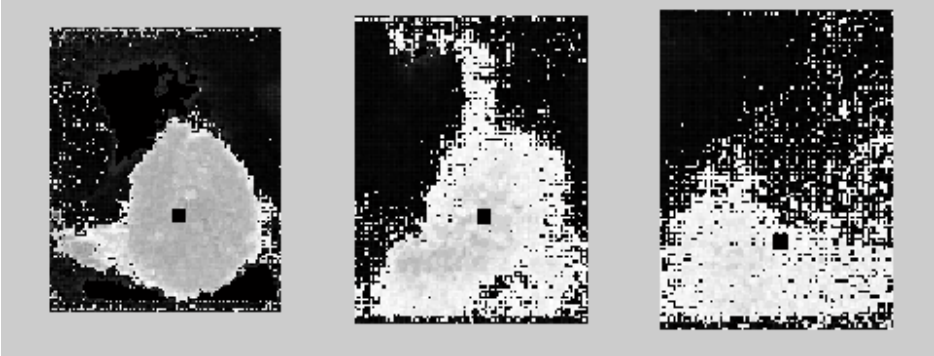

Figure 5.42 – Calculated centers for the three blue whirls of Picture 6 using the preliminary method

In this new case, instead of calculating the center from the black and white binary image, the method is going to use the grayscale image of the whirl. Hence, different weights can be assigned to the pixels depending on the value they have. Of course, those values are included in the [0,1] interval. But before calculating anything, a quality improvement can be performed. As it could be observed in Figure 5.42, there are a lot of pixels spread far from the whirl's actual center. This is a result of the non-perfect method utilized to convert the color images to the grayscale ones. However, if those pictures are transformed to black and white and a morphological opening and closing are performed, those pixels can be removed. Note that as a consequence, the result image is black and white, something that was not desirable for the current method where the pixels were supposed to be grayscale. But that was not a problem because the processed black and white image of the whirl (Figure 5.43) could be used as a mask for the grayscale original picture. Now, the result is a grayscale image similar to the first one but the undesired pixels have been removed (Figure 5.44).

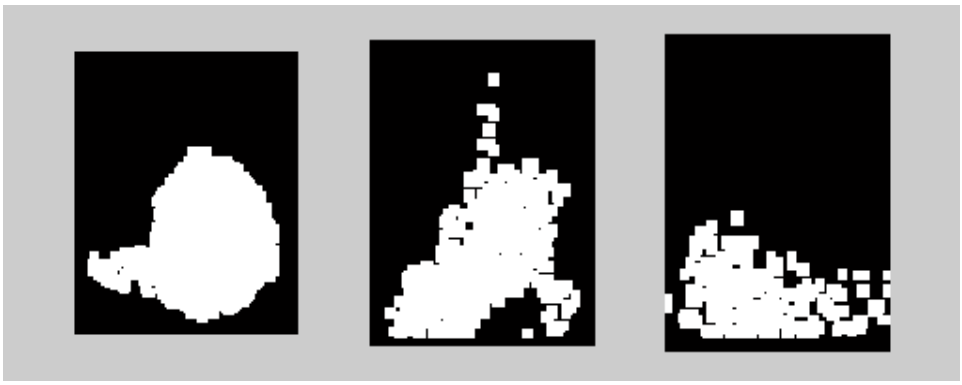

Figure 5.43 – The three black and white blue whirls of Picture 6 after morphological operations

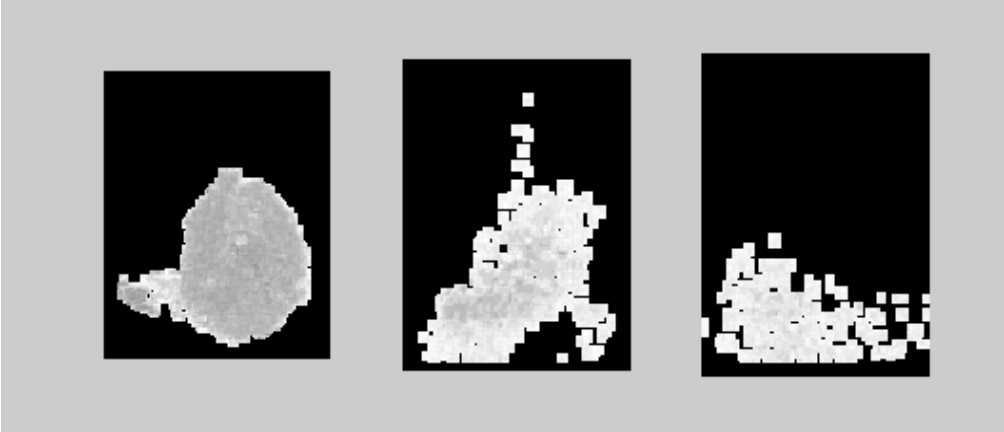

Figure 5.44 – Grayscale image of the three blue whirls of Picture 6 after applying the mask

The formula that was used in order to calculate the center of gravity is:

$$\overline{x} = \frac{1}{N} * \frac{1}{p_{avg}} * \sum_{y=1}^{y_{size}} \sum_{x=1}^{x_{size}} x * p(y,x)$$

$$\overline{y} = \frac{1}{N} * \frac{1}{p_{avg}} * \sum_{y=1}^{y_{size}} \sum_{x=1}^{x_{size}} y * p(y,x)$$

Where N is the total number of pixels in the picture, x_size and y_size are the total number of columns and rows, p(i) is the value of each pixel, p_avg is the average value of a pixel in the picture, and x and y are the coordinate values of each of the analyzed pixels. The final results can be observed on Figure 5.45.

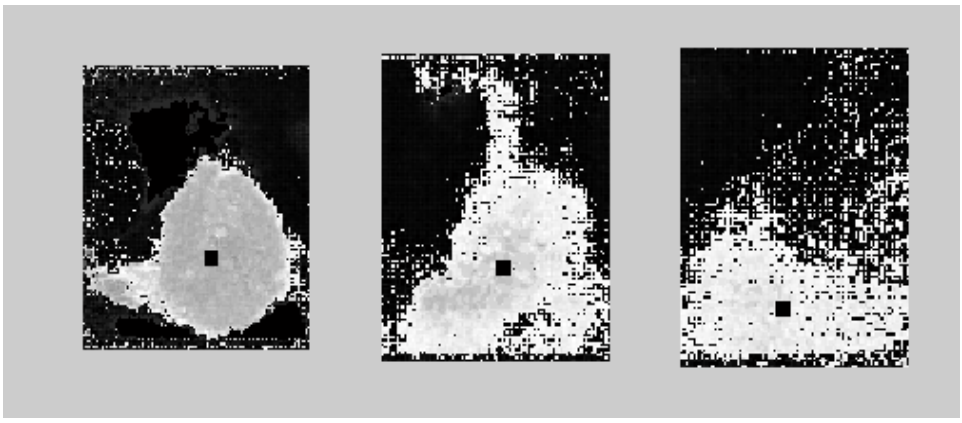

Figure 5.45 – Calculated centers for the three blue whirls of Picture 6 with the improved method

It is straightforward to conclude that this last method was much better than the old one. This technique still works for the "easy" rounded/squared whirls but it also gives the chance to obtain a really good approximation of the more complicated ones.

6. RESULTS

After all the process explained above, it is time to present the final results. The most important steps were the separation of the vortices on independent pictures and the calculation of the center of gravity of each of them. On Figure 6.1 these centers of gravity can be seen with red and blue dots. It is important to notice that with the previous algorithm the calculation of the center of gravity was not as accurate as desirable, and improvements were designed as explained on previous sections. In addition to that, other problems and bugs were fixed in order to make this algorithm work for these two set of pictures.

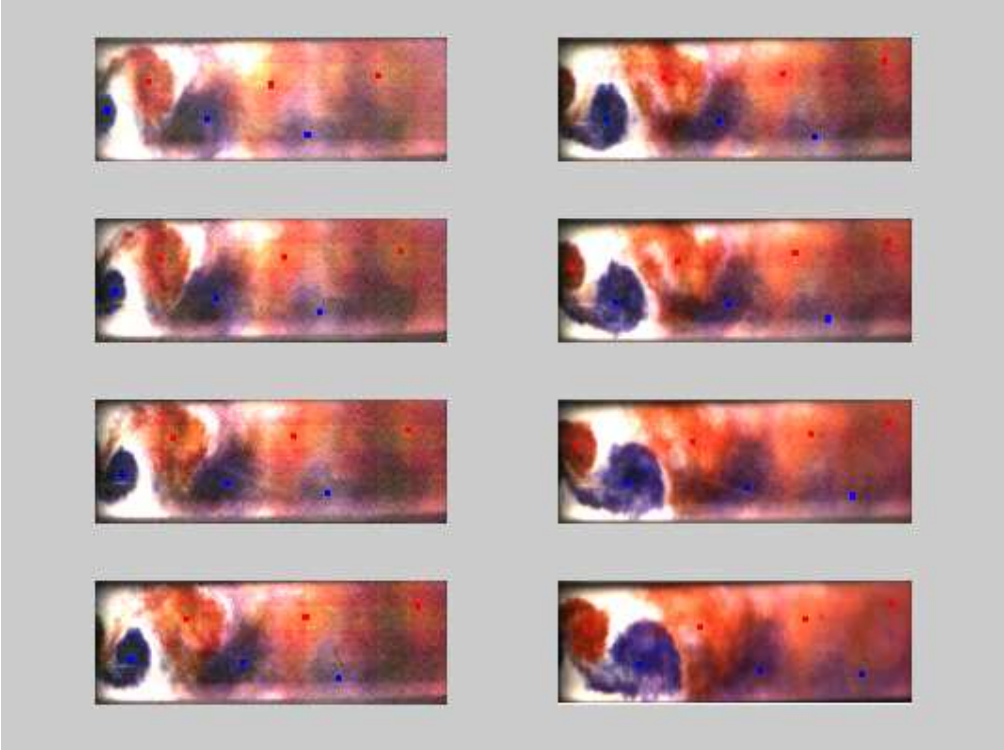

Figure 6.1 – Centers of gravity for all the whirls. Pictures 1-8

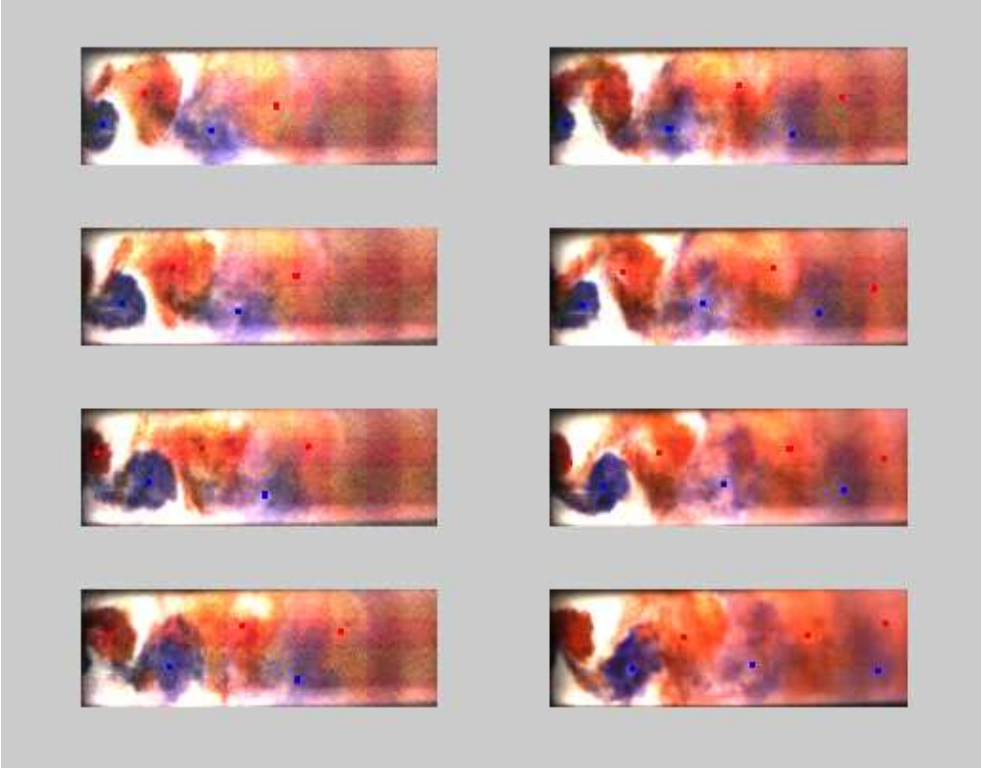

Figure 6.2 – Centers of gravity for all the whirls. Pictures 9-16

6.1 VORTICES' TRAJECTORY

The trajectory of the whirls is the first piece of information that can be obtained from the knowledge of the centers of gravity. Each of the following figures represents the trajectory of the blue or red whirls for a single set of pictures. Note that each of the whirls is represented with a different color, and below the trajectory points it is written which one of the whirls they represent. It has been considered the first whirl the one that arrived first (the furthest to the bluff body) and the following ones the ones that arrived later (the whirls obviously move from left to right). There are also numbers above some of the points that represent the time step where that specific point was observed, being time 1 the moment when Picture 1 was taken, time 2 the moment when Picture 2 was taken and so on. In each of the Figures it is represented the first time when a whirl was found (normally 1, meaning it appeared from time 1) and the last time that the whirl is seen (normally 8, meaning the whirl was detected till the last picture). For example, on Figure 6.3, we have three whirls in the image all the time from the first picture (time 1) to the last picture (time 8). If initially less whirls are detected and a new one shows up late from the bluff body (as the fourth whirl of Figure 6.4) the moment when it appears is also specified.

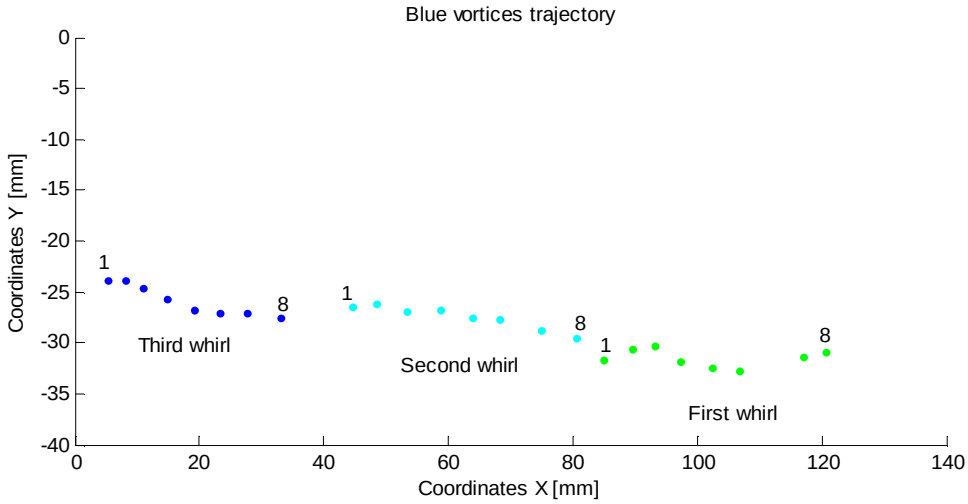

Figure 6.3 – Trajectory of the blue vortices on Pictures 1-8

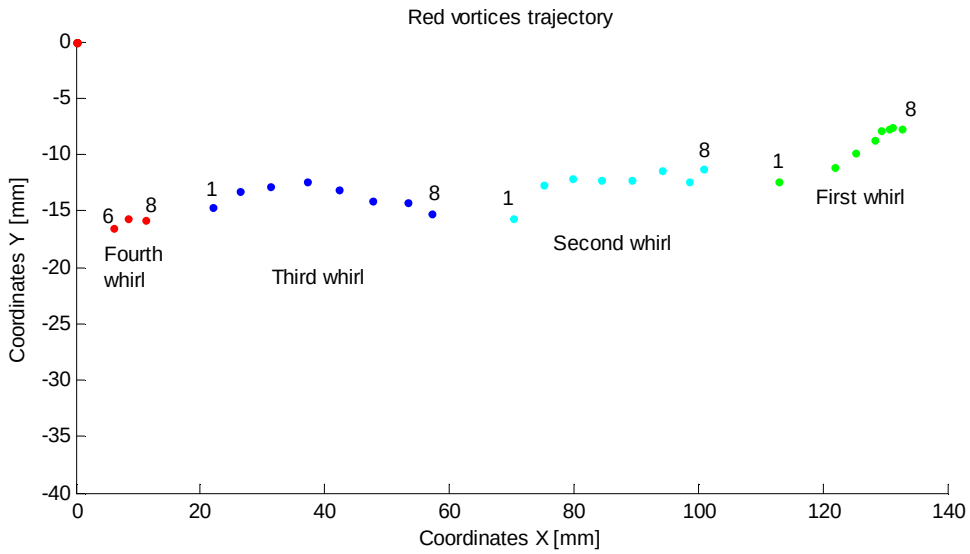

Figure 6.4 – Trajectory of the red vortices on Pictures 1-8

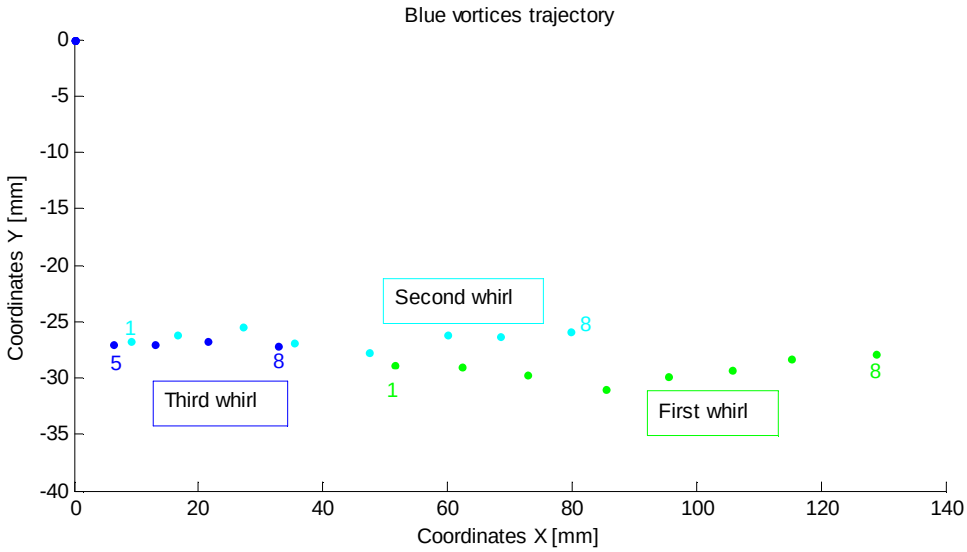

Figure 6.5 - Trajectory of the blue vortices on Pictures 9-16

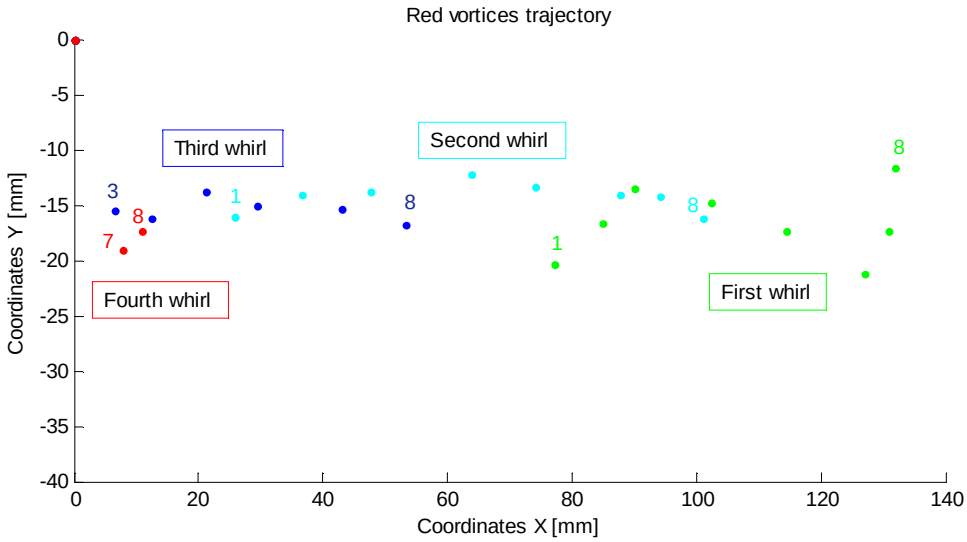

Figure 6.6 - Trajectory of the red vortices on Pictures 9-16

Interesting results can be obtained from these graphs, especially on the ones related to the first set of pictures. In Figure 6.3 and Figure 6.4, the trajectory of the whirls is very easy to follow. The blue whirls start a little bit under the bluff body and they keep going forward but not in a straight line, they separate from the middle axis with a certain angle. The same thing can be said from the red whirls, they start a little bit over the bluff body and then they move to the right with a little inclination from the axis. As it was expected, the centers of gravity calculated on the very far right side of the picture (specially the red ones) were not very accurate because of the blurriness and the poor quality, so those points should not be taken very much into account.

6.2 CONVECTION VELOCITY

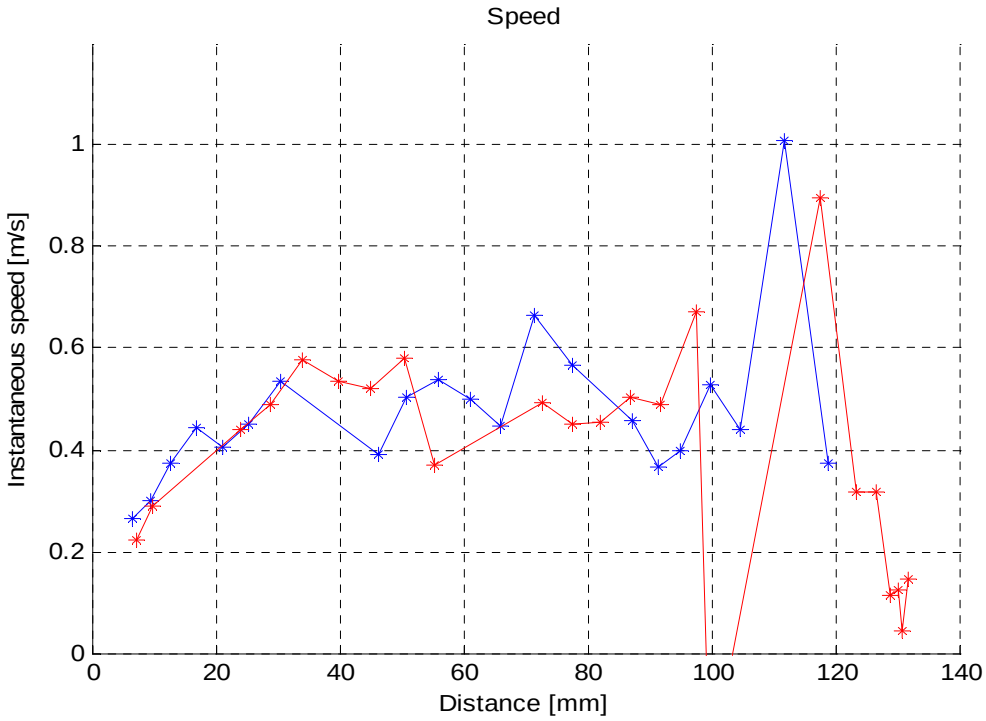

Figure 6.7 – Convection velocity for red and blue whirls on Pictures 1-8

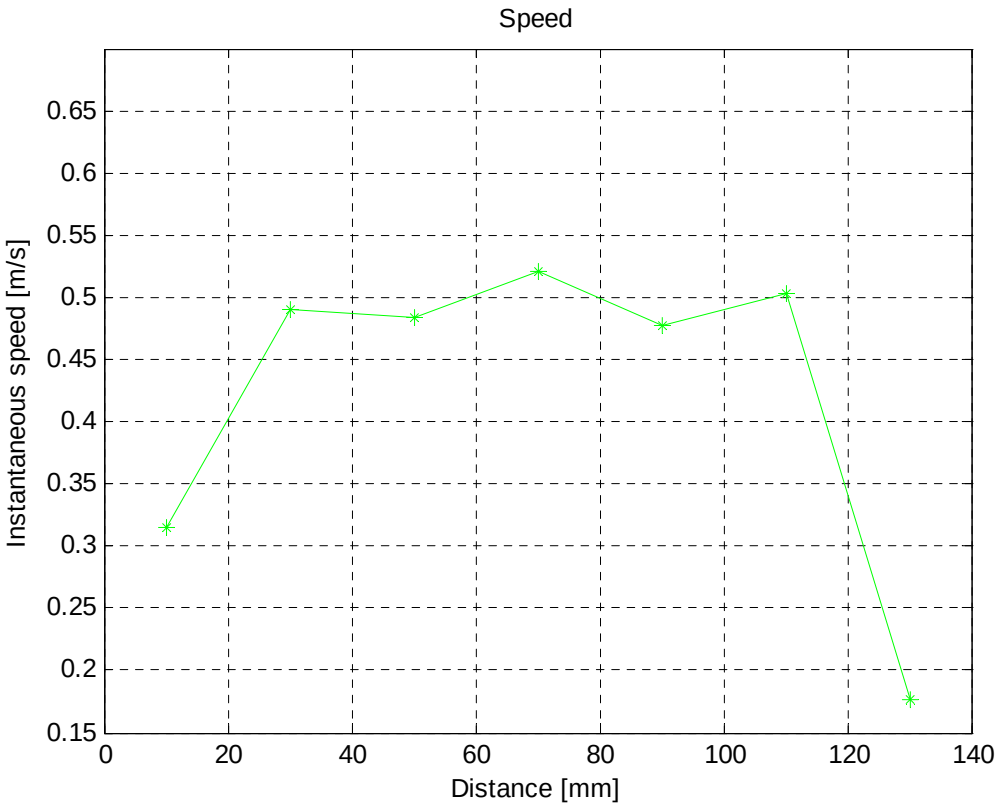

Figure 6.8 - Convection velocity vs distance from the bluff body on Pictures 1-8

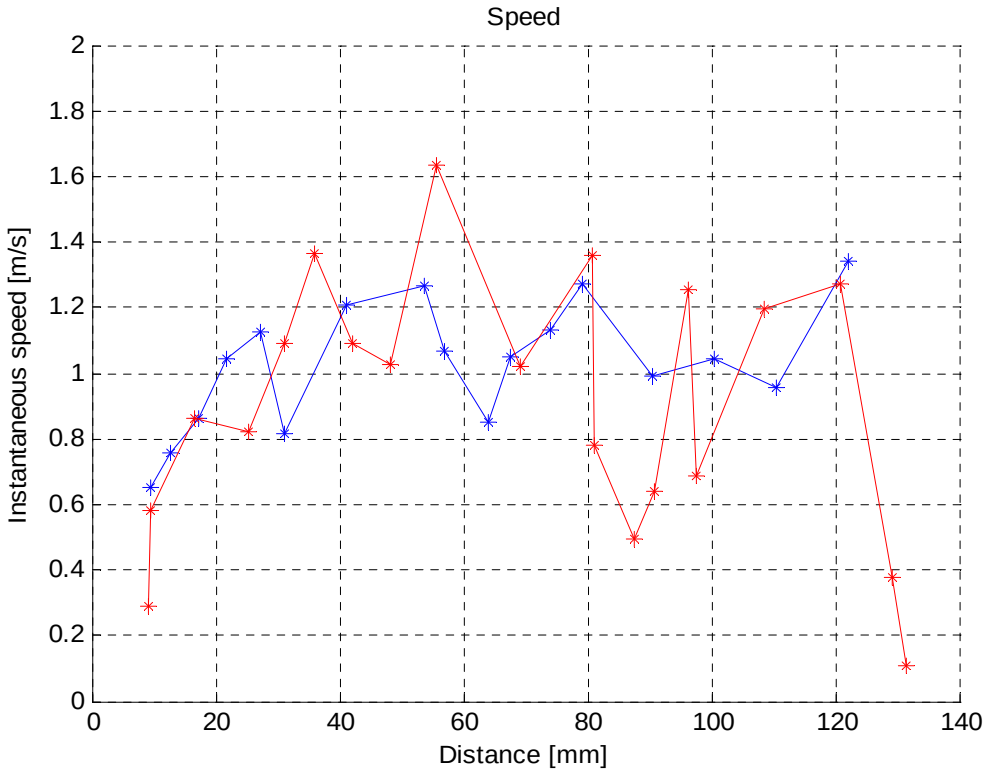

Figure 6.9 - Convection velocity for red and blue whirls on Pictures 9-16

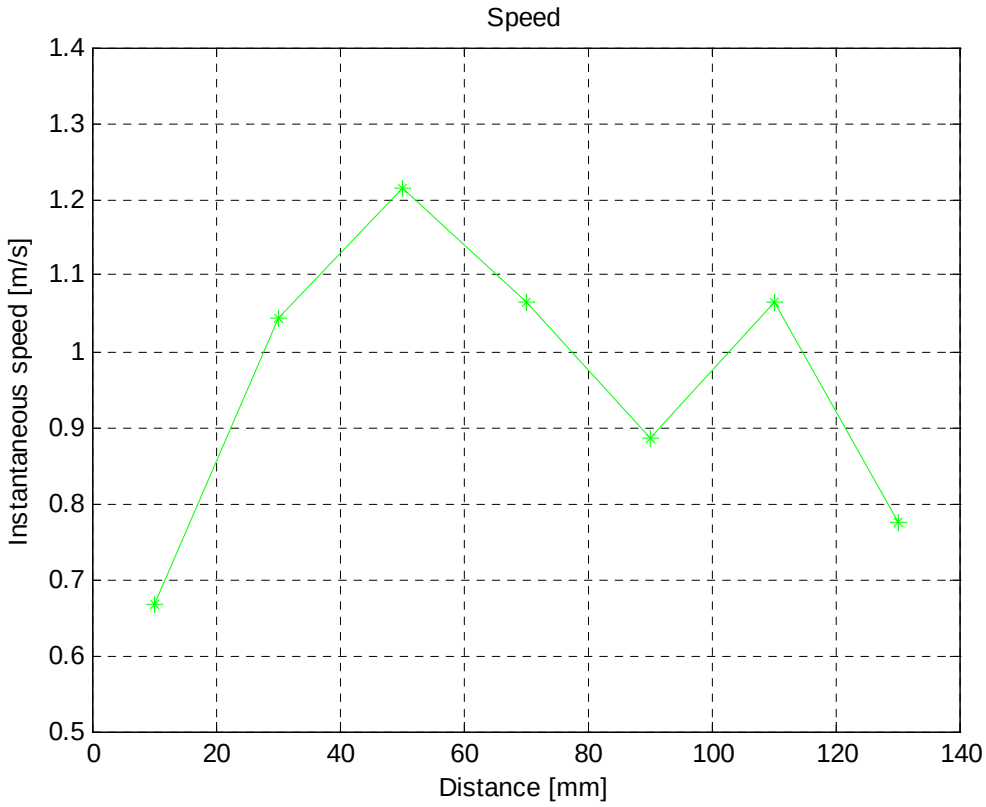

Figure 6.10 - Convection velocity vs distance from the bluff body on Pictures 9-16

The last result that was obtained from the investigation was the convection velocity of the vortices. The convection velocity was calculated in each of the points calculating the distance between the positions of the vortices between two consecutive pictures and dividing it by the time step.

Two kinds of graphs are presented in order to show the results. The first graphics (Figure 6.7 and Figure 6.9) show the convection velocity of the blue and the red whirls separately. There, it is possible to observe how the convection velocity of the vortices starts increasing in the proximity of the bluff body, but then it tends to become steady when it gets further. As a consequence of the imperfect calculation of the red centers of gravity, the variance in the steady zone is greater than for the blue ones. Also, once again, the values calculated for the right side of the pictures are not as valid as the previous ones, due to the reasons previously detailed in this report

The second graphs (Figure 6.8 and Figure 6.10) show the same results in a different way. For these plots, the average value of the convection velocity is calculated each 10 millimeters. Both “blue velocity” and “red velocity” are taken into account for the calculation.

These results match pretty well with the results obtained in previous investigations (Figure 3.3). If the last 25 millimeters of the pictures are neglected, the same conclusions are obtained, noticing that the convection velocity of the vortices is not constant and it is lower close to the bluff body.

7. CONCLUSIONS

Although the investigation of Kármán vortex street is and has been a difficult task throughout history, important results have been obtained by several scientists. In this investigation, after taking the pictures and processing them, several conclusions have been obtained.

The first one is that the quality of the pictures is crucial to be successful in the analysis. The nature of hydrodynamic phenomena and the applied method of visualization make the job very complicated, so a reliable image has to be taken in order to make a correct process. In this case, the right part of the images were not as clear as expected so the results obtained there are not valid to be taken into account

After obtaining the results, the vortices trajectory could be observed. The whirls that start above the bluff body tend to move towards the top of the tube, and the ones that start below the body tend to move towards the bottom. The convection velocity of the whirls was also calculated and those results confirmed the previous data obtained on the previous investigations. The theory that in the close neighborhood of the bluff body the vortices move slower than at a greater distance from their origin was confirmed.

Therefore, the objective of the project was achieved, confirming the previous investigations results and fixing and improving the algorithm given to the author.

8. REFERENCES

[1] Grzegorz L. Pankanin, Artur Kulińczak, Jerzy Berliński: "Investigations of Karman vortex street using flow visualization and image processing", *ScienceDirect*

[2] Pankanin G.L., Berliński J., Chmielewski R.: "Analytical modelling of Karman vortex street", *Metrology & Measurement Systems,* vol. XII, No 4, pp. 411-425, 2005.

[3] Pankanin G.L., Berliński J., Chmielewski R.: "Simulation of Karman vortex street development using new model", *Metrology & Measurement Systems,* vol. XIII, No 1, pp. 35-47, 2006.

[4] Birkhoff G.: "Formation vortex street", *Journal of Applied Physics* 24, No 1 (1953), pp. 98-103

[5] Birkhoff G., Zarantonello E.H., *Jets Wakes and Cavities*, Academic Press Inc. New York, 1957

[6] Funakawa M., "The Vibration of a Cylinder Caused by Wake Force in a Flow", *The Japan Society of Mechanical Engineers*, vol. 12, No. 53, 1969, pp. 1003-1010

[7] Pankanin G., Kulińczak A., Berliński J.: "Investigations of Karman Vortex Street Using Flow Visualization and Image Processing", *Sensors and Actuators A: Physical,* 138, pp. 366-375, 2007.

[8] Nakayama, Y. , Aoki, K.: "Progress of visualization", *Journal of Visualization, Vol. 4, No. 1 (2001) 9-18*

[9] Nobuyuki Otsu: "A Threshold Selection Method from Gray-Level Histograms", *IEEE Transactions on systems, man, and cybernetics, vol. smc-9, no. 1, January 1979*

[10] Grzegorz L. Pankanin, Artur Kulińczak: "Determination Of Vortex Convection Velocity With Application Of Flow Visualization And Image Processing" *XIX IMEKO World Congress Fundamental and Applied Metrology September 6−11, 2009, Lisbon, Portugal*

9. APPENDIX (matlab code)

```
function process(set_images)

%% This function processes one set of 8 pictures and shows the centers %% of
gravity, trajectory and convection velocity of the whirls found %% in those
pictures %%

%% INPUT: Set of pictures desired to be analyzed (1 (1-8) or 2 (9-16)

close all

%%%%%%%%%%%%%%%%%%%%%%%%%%%%%%%%%%%%%%%%%%%%%%%%%%%%%%%%%%%%%%%%%%%%%%%%%%%
%%%%%%%%%%%%%%%%PROCESSING THE MAGES%%%%%%%%%%%%%%%%%%%%%%%%%%%%%%%%%%%%%%%
%%%%%%%%%%%%%%%%%%%%%%%%%%%%%%%%%%%%%%%%%%%%%%%%%%%%%%%%%%%%%%%%%%%%%%%%%%%

%% obtaining images %%
if set_images == 1
     images = {imread('1.bmp'), imread('2.bmp'), imread('3.bmp'),
     imread('4.bmp'), imread('5.bmp'), imread('6.bmp'), imread('7.bmp'),
     imread('8.bmp')};
else
     images = {imread('9.bmp'), imread('10.bmp'), imread('11.bmp'),
     imread('12.bmp'), imread('13.bmp'), imread('14.bmp'),
     imread('15.bmp'),imread('16.bmp')};
end

%% getting configuration %%
temp = getConfig;
[pictNum imWidthMM imHeightMM time mark components] = temp{:};

%% imshow preferences %%
iptsetpref('ImshowBorder','tight');

%% obtaining blue (H component) and red (S-H component)
for i = 1:pictNum
     imgComp{i} = {readHsv(images{i},components(1)),
     readHsv(images{i},components(2))- readHsv(images{i},components(1))};
end

%% calculating centers of gravity %%
for i = 1:pictNum
   for col = 1:2
       c = process_picture(imgComp{i}{col},col);
       centers{i,col} = c;
   end
end

%% looking for possible missing centers %%
for i = 2:(pictNum-1)
    for col = 1:2
        n1 = size(centers{i-1,col},1);
        n2 = size(centers{i,col},1);
        n3 = size(centers{i+1,col},1);
        if (n2 < n3) && (centers{i+1,col}(1,2)>21)
             centers{i,col}(n2+1,1)= (centers{i-1,col}(n1,1) +
             centers{i+1,col}(n3,1))/2;
             centers{i,col}(n2+1,2)= (centers{i-1,col}(n1,2) +
             centers{i+1,col}(n3,2))/2;
        end
    end
end
```

```
%%%%%%%%%%%%%%%%%%%%%%%%%%%%%%%%%%%%%%%%%%%%%%%%%%%%%%%%%%%%%%%%%%%%%%%%%%%%
%%%%%%%%%%%%%%%%SHOWING THE RESULTS%%%%%%%%%%%%%%%%%%%%%%%%%%%%%%%%%%%%%%%%%%
%%%%%%%%%%%%%%%%%%%%%%%%%%%%%%%%%%%%%%%%%%%%%%%%%%%%%%%%%%%%%%%%%%%%%%%%%%%%%

%% SHOWING CENTERS OF GRAVITY (FIGURE 1) ---------------------------- %%

%% creating the empty figure %%
a=figure;
set(a,'ToolBar','none');

%% preparing the location of the dots %%
for i=1:pictNum
    for col=1:2
        for ser=1:size(centers{i,col},1)
             M=round([centers{i,col}(ser,1)-
             floor(mark/2),centers{i,col}(ser,2)-floor(mark/2)]);
                for j = M(1):M(1)+mark
                    for k = M(2):M(2)+mark
                        switch col
                            case 1
                                images{i}(j,k,:) = [0,0,255];   % blue dot
                            case 2
                                images{i}(j,k,:) = [255,0,0];   % red dot
                        end
                    end
                end
        end
    end

    %% preparing the final figure %%
    switch i
        case 1
            pos = 1;
        case 2
            pos = 3;
        case 3
            pos = 5;
        case 4
            pos = 7;
        case 5
            pos = 2;
        case 6
            pos = 4;
        case 7
            pos = 6;
        case 8
            pos = 8;
    end

    subplot(4,2,pos);
    imshow(images{i});
end

%% SHOWING WHIRLS VELOCITY (FIGURES 2 & 3) ------------------------- %%

%% calculating the modifiers between pixels and milimeters %%
modif = double(imWidthMM)/double(size(imgComp{1}{1},2));    % width modifier
modifY = double(imHeightMM)/double(size(imgComp{1}{1},1));  % height modifier

%% zero padding center matrix %%
whirls_num(1) = size(centers{pictNum,1},1); %maximum number of blue whirls
whirls_num(2) = size(centers{pictNum,2},1); %maximum number of red whirls
for col = 1:2
    for i = 1:pictNum
        if (whirls_num(col) - size(centers{i,col},1)) == 1
            for j = whirls_num(col):-1: 2
                centers{i,col}(j,:) = centers{i,col}(j-1,:);
            end
```

```
            centers{i,col}(1,:) = 0;
        elseif (whirls_num(col) - size(centers{i,col},1)) == 2
            for j = whirls_num(col):-1:3
                centers{i,col}(j,:) = centers{i,col}(j-2,:);
            end
            centers{i,col}(1,:) = 0;
            centers{i,col}(2,:) = 0;
        end
    end
end

%% calculating the velocity and position matrices %%

for col = 1:2
    for j = 1:whirls_num(col)
        for i = pictNum:-1:2
            if (centers{i,col}(j,1) ~= 0) && (centers{i-1,col}(j,1) ~= 0)
                    V{col}(j,i-1) = ((centers{i,col}(j,2) - centers{i-
                    1,col}(j,2))/time)*modif;
                    M_avg{col}(j,i-1) = ((centers{i,col}(j,2) + centers{i-
                    1,col}(j,2))/2)*modif;
            end
        end
    end
end


%% put the vectors in order %%

for col = 1:2
    M_avg_total{col} = [];
    V_total{col} = [];
    for j = 1:size(M_avg{col},1)
        for i = 1:(pictNum-1)
            if (M_avg{col}(j,i)~=0)
                M_avg_total{col} = [M_avg_total{col} M_avg{col}(j,i)];
                V_total{col} = [V_total{col} V{col}(j,i)];
            end
        end
    end
end

for col = 1:2
    for i = 1:(size(M_avg_total{col},2)-1)
        if M_avg_total{col}(i) > M_avg_total{col}(i+1)
            temp = M_avg_total{col}(i);
            temp2 = V_total{col}(i);
            M_avg_total{col}(i) = M_avg_total{col}(i+1);
            V_total{col}(i) = V_total{col}(i+1);
            M_avg_total{col}(i+1) = temp;
            V_total{col}(i+1) = temp2;
            for j = i:-1:1
                if M_avg_total{col}(j) >= M_avg_total{col}(j-1)
                    break;
                else
                    temp = M_avg_total{col}(j);
                    temp2 = V_total{col}(j);
                    M_avg_total{col}(j) = M_avg_total{col}(j-1);
                    V_total{col}(j) = V_total{col}(j-1);
                    M_avg_total{col}(j-1) = temp;
                    V_total{col}(j-1) = temp2;
                end
            end
        end
    end
end
```

```
%% take the average values of the red and blue whirls %%

M_final = [10 30 50 70 90 110 130];
for i = 1:7
    V_sectors{i} = [];
end

for col = 1:2
    for i = 1:size(M_avg_total{col},2)
        if M_avg_total{col}(i) < 20
            V_sectors{1} = [V_sectors{1} V_total{col}(i)];
        elseif M_avg_total{col}(i) < 40
            V_sectors{2} = [V_sectors{2} V_total{col}(i)];
        elseif M_avg_total{col}(i) < 60
            V_sectors{3} = [V_sectors{3} V_total{col}(i)];
        elseif M_avg_total{col}(i) < 80
            V_sectors{4} = [V_sectors{4} V_total{col}(i)];
        elseif M_avg_total{col}(i) < 99
            V_sectors{5} = [V_sectors{5} V_total{col}(i)];
        elseif M_avg_total{col}(i) < 120
            V_sectors{6} = [V_sectors{6} V_total{col}(i)];
        else
            V_sectors{7} = [V_sectors{7} V_total{col}(i)];
        end
    end
end

for i = 1:7
    V_final(i) = mean(V_sectors{i});
end


%% plot the red and blue whirls velocity separately %%
a=figure;
set(a,'ToolBar','none');
hold on;

for col = 1:2
    if (col == 1)
        plot(M_avg_total{col},V_total{col},'b*-');
    else
        plot(M_avg_total{col},V_total{col},'r*-');
    end
end

grid on;
if set_images == 1
    axis([0 imWidthMM 0 1.2]);
else
    axis([0 imWidthMM 0 2]);
end
ylabel('Instantaneous speed [m/s]');
xlabel('Distance [mm]');
title('Speed');
hold off;

%% plot the average of the red and blue whirls velocity %%

a=figure;
set(a,'ToolBar','none');
plot(M_final,V_final,'g*-');
grid on;
if set_images == 1
    axis([0 imWidthMM 0.15 0.7]);
else
    axis([0 imWidthMM 0.5 1.4]);
end
ylabel('Instantaneous speed [m/s]');
```

```
xlabel('Distance [mm]');   %distance
title('Speed');


%% SHOWING WHIRLS TRAJECTORY (FIGURES 5 & 6) ----------------------- %%

%% blue whirls trajectory %%
a=figure;
set(a,'ToolBar','none');
set(a,'Color',[1 1 1]);
hold on;
for pic = 8:-1:1
    cent_mm = centers{pic,1};
    cent_mm(:,1) = cent_mm(:,1)*modifY*(-1);
    cent_mm(:,2) = cent_mm(:,2)*modif;
    index=0;
    for c=size(centers{pic,1},1):-1:1
        index=index+1;
        switch index
            case 1
                color = 'g.-';
            case 2
                color = 'c.-';
            case 3
                color = 'b.-';
            case 4
                color = 'r.-';
        end
        plot(cent_mm(c,2),cent_mm(c,1),color);
    end
end
title('Blue vortices trajectory');
axis([0 imWidthMM -imHeightMM 0]);
ylabel('Coordinates Y [mm]');   %Y coordinate
xlabel('Coordinates X [mm]');   %X coordinate
hold off;

%% red whirls trajectory %%
a=figure;
set(a,'ToolBar','none');
set(a,'Color',[1 1 1]);
hold on;
for pic = 8:-1:1
    cent_mm = centers{pic,2};
    cent_mm(:,1) = cent_mm(:,1)*modifY*(-1);
    cent_mm(:,2) = cent_mm(:,2)*modif;
    index=0;
    for c=size(centers{pic,2},1):-1:1
        index=index+1;
        switch index
            case 1
                color = 'g.-';
            case 2
                color = 'c.-';
            case 3
                color = 'b.-';
            case 4
                color = 'r.-';
        end
        plot(cent_mm(c,2),cent_mm(c,1),color);
    end
end
title('Red vortices trajectory');
axis([0 imWidthMM -imHeightMM 0]);
ylabel('Coordinates Y [mm]');   %Y coordinate
xlabel('Coordinates X [mm]');   %X coordinate
hold off;
```

```
function I = readHsv(img,comp)

%% function for obtaining the HSV components %%
%% INPUT:  RGB image and desired HSV component (1-H 2-S)
%% OUTPUT: desired HSV component

temp = rgb2hsv(img);
I = temp(:,:,comp);


function conf=getConfig()

%% function for getting the configuration values from conf.txt file

confFile = fopen('conf.txt','r');
conf = textscan(confFile,'%d%f%f%f%d%s','delimiter',';','headerlines',8);
conf{6}=str2num(char(conf{6}));
```

```
function [C]=process_picture(img,col)

%% function for processing single images %%
%% INPUT:  Current HSV component image, color
%% OUTPUT: matrix with row and column of the center positions of the whirls

tol = 8;           % tolerance of dividers location

%% getting new dividers %%
divsClear = get_divider(img,col);

if (divsClear == 0)
    % didn't find any whirls
    C = 0;
    return;
end

%% add tolerance %%
for i=1:size(divsClear,1)

    if(divsClear(i,1)<tol+1)
        divsClear(i,1)=1;
    else
        divsClear(i,1)=divsClear(i,1)-tol;
    end

    if(divsClear(i,2)+tol>size(img,2))
        divsClear(i,2)=size(img,2);
    else
        divsClear(i,2)=divsClear(i,2)+tol;
    end
end

for i=1:size(divsClear,1)

    %% cut out small image of object %%
    imgCut = img(:,divsClear(i,1):divsClear(i,2));

    %% get center location %%
    C(i,:) = get_center(imgCut);

    %% add offset %%
    C(i,2) = C(i,2) + divsClear(i,1);
end
```

```
function [dividers] = get_divider(img,col)

%% function for obtaining the start and end points of the whirls in an image%%
%% INPUT:  Current HSV component image, color
%% OUTPUT: matrix with row and column of the dividers locations

%% conversion to blackwhite %%
level = graythresh(img);    % matlab default Otsu thershold
imBW = im2bw(img,level);

if (col == 1)   % for blue whirls

    %% morphological opening and closing %%
    imBWO = imopen(imBW,ones(4));
    imBWOC = imclose(imBWO,ones(4));

    %% fill holes %%
    imBWOCF = bwfill(imBWOC,'holes',8);

    %% aggresive open for small part deletion %%
    imBWOCFO = imopen(imBWOCF,ones(9));

    %% blackwhite label %%
    [imgLabel,labNum] = bwlabel(imBWOCFO,8);

    %% clear small parts %%
    do = 1;
    while(do)
        [imgLabel,labNum] = bwlabel(imgLabel,8);
        if (labNum == 0)
            dividers = 0;
            return;
        end
        for i=1:labNum
            area = bwarea(imgLabel==i);
            if(area<400)
                cells=find(imgLabel==i);
                imgLabel(cells)=0;
                imBWOCFO(cells)=0;
                break;
            end
            if (i==labNum)
                do=0;
            end
        end
    end

    for i=1:labNum
        [tmp,dividers(i,1)] = find(imgLabel==i,1,'first');
        [tmp,dividers(i,2)] = find(imgLabel==i,1,'last');
    end


elseif (col == 2)   % for the red whirls

    %% division of the picture into two parts %%
    div = floor(size(img,2)/4);
    imBW1 = imBW(:,1:div);
    imBW2 = imBW(:,div+1:size(img,2));

    %% first part ------------------------------------------------- %%

    %% morphological opening and closing %%
    imBWO1 = imopen(imBW1,ones(3));
    imBWOC1 = imclose(imBWO1,ones(3));

    %% fill holes %%
    imBWOCF1 = bwfill(imBWOC1,'holes',8);
```

```
        %% aggresive open for small part deletion %%
        imBWOCFO1 = imopen(imBWOCF1,ones(6));

        %% second part ------------------------------------------------- %%
        %% morphological opening and closing %%
        imBWO2 = imopen(imBW2,ones(5));
        imBWOC2 = imclose(imBWO2,ones(5));

        %% fill holes %%
        imBWOCF2 = bwfill(imBWOC2,'holes',8);

        %% aggresive open for small part deletion %%
        imBWOCFO2 = imopen(imBWOCF2,ones(10));

        %% two parts together ------------------------------------------ %%
        imBWOCFO = [imBWOCFO1 imBWOCFO2];

        %% blackwhite label %%
        [imgLabel,labNum] = bwlabel(imBWOCFO,8);

        %% clear small parts %%
        do = 1;
        while(do)
            [imgLabel,labNum] = bwlabel(imgLabel,8);
            if (labNum == 0)
                dividers = 0;
                return;
            end
            for i=1:labNum
                area = bwarea(imgLabel==i);
                if(area<650)
                    cells=find(imgLabel==i);
                    imgLabel(cells)=0;
                    imBWOCFO(cells)=0;
                    break;
                end
                if (i==labNum)
                    do=0;
                end
            end
        end

        for i=1:labNum
            [tmp,dividers(i,1)] = find(imgLabel==i,1,'first');
            [tmp,dividers(i,2)] = find(imgLabel==i,1,'last');
        end

        %% correcting centers when big whirls are found %%
        subs = dividers(:,2)-dividers(:,1);
        for i=1:labNum
            if subs(i) > 2/3*size(img,2)
                temp = dividers (i,2);
                dividers(i,2) = dividers(i,1) + floor(subs(i)/3);
                dividers(i+1,1) = dividers(i,2) + 1;
                dividers(i+1,2) = dividers(i,1) + 8*floor(subs(i)/9);
                dividers(i+2,1) = dividers(i+1,2) + 1;
                dividers(i+2,2) = temp;

            elseif (subs(i) > 0.4*size(img,2))&&(subs(i) < 2/3*size(img,2))
                temp = dividers (i,2);
                dividers(i,2) = dividers(i,1) + 3*floor(subs(i)/4);
                dividers(i+1,1) = dividers(i,2) + 1;
                dividers(i+1,2) = temp;
            end
        end

    end
```

```
function [C] = get_center(imgCut)

%% function calculating mass centers of the object
%% INPUT:  grayscale, cutout object
%% OUTPUT: center location

level = graythresh(imgCut);
imBW = im2bw(imgCut,level);

%% morphological opening and closing %%
imgOpen = imopen(imBW,ones(4));
imgClose = imclose(imgOpen, ones(1));

%% applying mask to the image %%
imgCut_mask = imgClose.*imgCut;

%% algorithm to look for the center ------------------------------------%%
x_size = size(imgCut,1);
y_size = size(imgCut,2);

%% calculating the mean value assigned to any pixel %%
N = x_size * y_size;
pix_avg=0;
for j=1:x_size
    for k=1:y_size
        pix_avg = pix_avg + imgCut_mask(j,k)/N;
    end
end

%% calculating the center of gravity %%
x_mean=0;
y_mean=0;
for j=1:x_size
    for k=1:y_size
        x_mean = x_mean + (1/N) * (1/pix_avg) * j * imgCut_mask(j,k);
        y_mean = y_mean + (1/N) * (1/pix_avg) * k * imgCut_mask(j,k);
    end
end
[C]=[x_mean,y_mean];
```